

T-2983

A STUDY OF THE STORAGE DEPOSIT  
OF A MODEL FUEL AND JET A FUEL

by

Wen-Chia Chen

ProQuest Number: 10782642

All rights reserved

INFORMATION TO ALL USERS

The quality of this reproduction is dependent upon the quality of the copy submitted.

In the unlikely event that the author did not send a complete manuscript and there are missing pages, these will be noted. Also, if material had to be removed, a note will indicate the deletion.



ProQuest 10782642

Published by ProQuest LLC (2018). Copyright of the Dissertation is held by the Author.

All rights reserved.

This work is protected against unauthorized copying under Title 17, United States Code  
Microform Edition © ProQuest LLC.

ProQuest LLC.  
789 East Eisenhower Parkway  
P.O. Box 1346  
Ann Arbor, MI 48106 – 1346

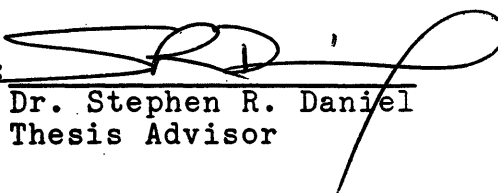
Submittal Sheet

A thesis submitted to the Faculty and the Board of Trustees of the Colorado School of Mines in partial fulfillment of the requirements for the degree of Master of Science (Chemistry).

Golden, Colorado

Date 9/13/85

Signed: Wen Chia Chen  
Wen-Chia Chen

Approved:   
Dr. Stephen R. Daniel  
Thesis Advisor

Golden, Colorado

Date: 9/13/85

George H. Kennedy  
Dr. George H. Kennedy  
Department Head  
Chemistry and Geochemistry

## ABSTRACT

In this study, a model system (1/10 ml, V/V, tetralin/ dodecane), developed from the previous studies in this laboratory, was analyzed together with the Jet A fuel system. Various techniques of instrumental analysis, including high performance liquid chromatography (HPLC), gas chromatography (GC), pyrolysis mass spectrometry (PY/MS), gas chromatography/ mass spectrometry (GC/MS), secondary ion mass spectrometry (SIMS), C-13 solid and liquid nuclear magnetic resonance spectroscopy (C-13 NMR), infrared spectrometry (IR), and elemental analysis, were applied for obtaining useful structural information for the model and the Jet A deposits. Wet chemistry functional group analysis and organic compound derivatization were also used to further understand the results obtained from the instrumental analyses. Column separation methods (eg. HPLC and open column) were developed in order to fractionate deposits prior to analysis thus simplifying the interpretation of mass spectra.

Deposits of the model system and the Jet A system were found to consist of more than one compound. The investigation of the model system revealed that it is not a straightforward system to work with. Its complexity

comes from the many oxidation products of tetralone and the diverse process by which they combine in an air environment to form deposits. Further understanding of the role of tetralin, tetralin hydroperoxide, and tetralone in the model deposit formation process helped to postulate the basis of formation of model deposit and of Jet A deposit. The integration of modern instrumental analyses indicates that aromatic, tetralone-like, fused ring compounds are a part of the model and Jet A deposits. N-dodecane is suspected of participation in the process of the deposit formation; however, further investigation is required. Condensation of the aromatic carbonyl plays an important role in deposit formation but the reaction is not as straightforward as was suggested in the previous work. Further oxidation beyond tetralone and tetralin hydroperoxide is required. Peroxy linkage was not observed in the designed experiment. While some difference in model and Jet A deposits were found, the two are markedly similar and tetralin/dodecane is a useful system for modeling the chemistry of deposit formation.

## TABLE OF CONTENTS

<u>Section</u>	<u>Page</u>
ABSTRACT .....	iii
LIST OF FIGURES .....	ix
LIST OF TABLES .....	xi
ACKNOWLEDGEMENTS .....	xii
INTRODUCTION .....	1
Background .....	1
Some Investigations of the Deposit Structure ...	4
Introduction to Secondary Ion Mass Spectrometry (SIMS) .....	10
Introduction to CP/MAS C-13 NMR .....	12
Introduction to Multiple Internal Reflectance Infrared (MIR-IR) .....	14
EXPERIMENTAL WORK .....	18
Preparation of Chemicals and Reagents .....	18
Instrumental Analyses .....	20
Other Analyses .....	23
The Preparation of the Jet A Deposit and the Model Deposit .....	23
Physical Properties of the Deposits .....	24
The Variation of Aliphatic Hydrogen and Aromatic Hydrogen Ratio in Aged Model Fuel .....	25
Dichloromethane and THF Extracts of Deposits ...	25
The Separation and Collection of the Components in the Dichloromethane Extract of the Model Deposit .....	26

<u>Section</u>	<u>Page</u>
Benzene and THF Extracts of Deposits .....	28
Group Separation by Open Column Chromatography of Model Deposit .....	28
Sample Preparation for SIMS Analysis .....	29
Sample Preparation for Carbon-13 NMR Analysis ..	29
Wet Chemical Analysis .....	30
Derivatives of 1-Tetralone and the Model Deposit	31
Detecting Peroxide Linkage in the Model Deposit	31
RESULTS AND DISCUSSION .....	32
Gel Permeation Chromatography (GPC) .....	32
High Performance Liquid Chromatography (HPLC) ..	32
Carbon, Hydrogen, and Nitrogen Analysis .....	32
Derivatives of 1-Tetralone and Model Deposit ...	36
Functional Group Investigation by Wet Chemical Techniques .....	36
The Test of the Peroxy Linkage in the Model Deposit .....	39
MIR-IR Analysis of Model deposit and Jet A Deposit .....	40
The Comparison of MIR-IR Analysis of the Benzene Extract and Benzene-insoluble/THF-soluble Fraction of the Model Deposit .....	42
The Comparison of MIR-IR Analysis of the Dichloro- methane Extract and Dichloromethane-insoluble/THF- soluble Fraction of the Model Deposit .....	45
Analysis of the Model Deposit Fractions Collected from HPLC .....	47

<u>Section</u>	<u>Page</u>
Conclusions from MIR-IR Analysis of the Model Deposit .....	50
The Comparison of MIR-IR Analysis of the Benzene Extract and the Benzene-insoluble/THF-soluble Fraction of the Jet A Deposit .....	50
The Comparison of MIR-IR Analysis of the Dichloroethane Extract and Dichloromethane-insoluble/THF-soluble Fraction of the Jet A Deposit .....	53
C-13 NMR Spectroscopy (Solution Phase, Deuterated Chloroform as Solvent) .....	53
Proton NMR .....	55
CP/MAS Solid State NMR .....	55
Secondary Ion Mass Spectrometry .....	59
Gas Chromatography/Mass Spectrometry .....	66
Pyrolysis Mass Spectrometric Analysis .....	66
PY/MS Analysis of the Benzene Extract of the Model Deposit .....	72
PY/MS Analysis of the Benzene-insoluble/THF-soluble Fraction of the Model Deposit .....	72
PY/MS Analysis of Benzene Extract of the Jet A Deposit .....	74
PY/MS Analysis of the Benzene-insoluble/THF-soluble Fraction of the Jet A Deposit .....	76
PY/MS Analysis of the Dichloromethane Extract of the Model Deposit .....	76
PY/MS Analysis of the Dichloromethane-insoluble/THF-soluble Fraction of the Model Deposit .....	78
CONCLUSIONS .....	79
REFERENCES .....	82

<u>Section</u>	<u>Page</u>
APPENDICES .....	85
Appendix 1. The Summary of the MIR-IR Analyses of the Deposits .....	86
Appendix 2. C-13 NMR Spectrum of the Model Deposit .....	88
Appendix 3. Sample Calculation of Har/Car and Hal/Cal .....	89
Appendix 4. The Mechanism of Tetralone Fragmentation in Mass Spectrometry .....	90
Appendix 5. PY/MS Data Files .....	91

## LIST OF FIGURES

<u>Figure</u>	<u>Page</u>
Figure 1. Basic Components of SIMS .....	11
Figure 2. (a) Total Reflectance (b) Multiple Internal Reflectance .....	16
Figure 3. HPLC Separation of the Model Deposit and the Jet A Deposit .....	33
Figure 4. MIR-IR Spectra of (a) Model Deposit (b) Jet A Deposit .....	41
Figure 5. MIR-IR Spectra of the Model Deposit (a) Benzene Extract (b) THF Fraction .....	43
Figure 6. MIR-IR Spectra of the Model Deposit (a) Dichloromethane Extract (b) THF Fraction	46
Figure 7. HPLC Separation of the Model Deposit, P2 and are P3 Two Fractions Collected from the HPLC	48
Figure 8. MIR-IR Spectra of the Model Deposit Fractions Collected from HPLC (a) P2 (b) P3 .....	49
Figure 9. MIR-IR Spectra of the Jet A Deposit (a) Benzene Extract (b) THF Fraction .....	51
Figure 10. MIR-IR Spectra of the Jet A Deposit (a) Dichloromethane Extract (b) THF Fraction	54
Figure 11. PNMR of the Model Deposit .....	58
Figure 12. CP/MAS Solid State NMR of the Model Deposit	60
Figure 13. CP/MAS Solid State NMR of the Jet A Deposit	61
Figure 14. SIMS Spectrum of the Model Deposit .....	62
Figure 15. SIMS Spectrum of the Jet A Storage Deposit	64
Figure 16. SIMS Spectrum of the Jet A Thermal Deposit (a) Initial (b) Final (10 min later) .....	65

<u>Figure</u>	<u>Page</u>
Figure 17. PY/MS Spectra of the Model Deposit (a) Benzene Extract (b) THF Fraction .....	73
Figure 18. PY/MS Spectra of the Jet A Deposit (a) Benzene Extract (b) THF Fraction .....	75
Figure 19. PY/MS Spectra of the Model Deposit (a) Dichloromethane Extract (b) THF Fraction	77

## LIST OF TABLES

<u>Table</u>		<u>Page</u>
Table 1.	CHN Analyses of the Model Deposit and Jet A Deposit from Previous Work (14) .....	9
Table 2.	MIR-IR Absorption Bands of the Model Deposit from Previous Work (14) .....	9
Table 3.	CHN Analyses of the Model Deposit and the Jet A Deposit and Some Known Compounds .....	35
Table 4.	The Melting Point of the Model Deposit and Several Pure Compounds .....	37
Table 5.	Summary of Wet Chemical Analyses .....	38
Table 6.	C-13 NMR Chemical Shifts Chosen from the Spectrum of the Model Deposit to Compare with the Literature Chemical Shift Values of Tetralone .....	56
Table 7.	Structural Parameters from NMR Analysis .....	57
Table 8.	The Possible Molecular Structures of the Oxidation Products from Tetralin and Tetralone	67
Table 9.	Mass Peaks in Spectra of Various Reference Compounds .....	71

### ACKNOWLEDGEMENTS

The author expresses gratitude to Dr. Stephen Daniel for his patience and guidance throughout this study. Appreciation is also given to Dr. George Lucas and Dr. Scott Cowley for serving on my committee. Appreciation is extended to Dr. Robert Orth, Dr. Marvin Curtis and Dr. Ru-Shung Tsao for performing analyses. Finally, I would like to thank the NASA Lewis Research Center for funding this research and the Colorado State University Regional NMR Center for performing C-13 solid state NMR analyses.

## INTRODUCTION

Background

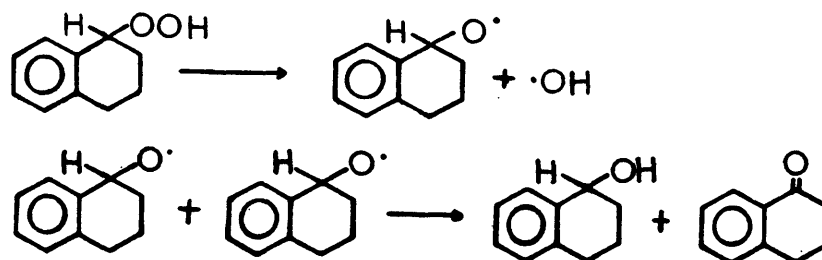
The consumption of Jet A fuel is estimated to have been 840,000 bbl/day in 1980 and is predicted to be 1,310,000 bbl/day by the year 2000 (1). To meet such a large demand, refiners are facing the challenge of maintaining the high quality requirements of jet fuel refined from crudes of diminishing quality. Because of the oil embargo of the 70's, a primary concern of the U.S. Department of Defense is the storage of adequate fuel supplies for emergency defense needs. The stability of fuel in storage is thus becoming an important issue. As a result, the Department of Defense initiated research projects to study alternative sources for transportation fuels - coal, oil shale, and tar sands (2). Jet fuel has been found to form insoluble deposits on heated surfaces and in storage tanks. Two types of deposits are categorized as storage and thermal deposits. The formation of storage deposits is believed to begin with the autoxidation of hydrocarbons while the fuel is stored in contact with air. Thermal deposits are formed on heated surfaces in an operating engine. In aircraft, the deposit formed on the surfaces of heat exchangers and in the fuel delivery system reduces

the efficiency of heat exchangers and clogs nozzles and filters. Sulfur and nitrogen compounds in fuels have been shown to decrease the stability of fuels and to be involved in the deposit formation processes (3). The concentrations of sulfur and nitrogen compounds are higher in the fuels from shale and coal than in fuels from crude oil (43). Removing these deleterious materials, mostly by hydrogenation, increases the price of the oil from shale and coal. The significance of these problems increases with the design of future engines to be operated at elevated temperatures.

Little structural information has been reported on either storage or thermal deposits from any distillate fuels. Clearly, these materials are structurally complex. However, such structural study has received more attention recently, because of advances in instrumentation and analytical techniques for solid samples. Mayo and Buttrill have reported Field Ionization Mass Spectrometry (FIMS) studies on fuel deposits (4). Seng and Helmick (5) have applied various instrumental analyses, Fourier Transform Infrared (FT-IR), Electron Spectroscopy for Chemical Analysis (ESCA), Scanning Electron Microscopy (SEM), Energy Dispersive Analysis of X-Ray (EDAX), Raman Spectroscopy, and Secondary Ion Mass Spectrometry (SIMS), photoacoustic

techniques, and Triple Quadrupole Mass Spectrometry, to study both thermal and storage deposits. The structural analysis of fuel deposits is at the beginning stage; no firm conclusions have yet been reached. Hence, even a little more understanding about the structure of fuel deposits would greatly aid in attacking the problem.

In previous work, the nitrogen, sulfur, and oxygen contents of the deposits were found to be greater than in the parent fuel (6). The oxygen involvement arises from air oxidation of the hydrocarbons (6,7,8,9). Morrell et al. (8) demonstrated that deposit formation in gasoline is directly related to hydroperoxide formation. Many mechanisms of hydroperoxide decomposition have been explored (10,11,12,13). Most commonly, the hydroperoxide disproportionates to form alcohols and ketones. For example,



The storage deposits of hydrocarbon fuels are only partially soluble in  $\text{CHCl}_3$ ,  $\text{CH}_2\text{Cl}_2$ , and *N,N*-dimethyl formamide (14). Because of their insolubility, good spectra are very dif-

difficult to obtain. However, aromatic C-H, carbonyl and hydroxyl groups have been identified in the deposits from various fuels (4,15,16,17). In accordance to the results from IR spectroscopy, Mayo (15) has suggested several classes of compounds which have the solubility characteristics of the pentane-soluble gums, where "gum" was the solid obtained by evaporating aged fuel.

- " a. compounds having bifunctional oxygen, molecular weights of a few hundred and carbonyl and hydroxyl groups
- b. polymers from condensation reactions of compounds with high molecular weight and moderate polarity
- c. metal complexes with these solubility characteristics of oxidation products of fuels are precursors for deposit formation and the functional groups containing oxygen are a part of the structure of deposit. "

#### Some Investigations of the Deposit Structure

Mayo has reported spectral analyses on n-decane oxidation products and jet fuel fractions in his earlier research work (15). Oxidation of n-decane was carried out in a Pyrex reactor at 155°C with a slow air stream passing through the reactor. The oxidation products were analyzed by IR, NMR, and mass spectrometry. The infrared data show strong ketone and alcohol absorptions and weak aldehyde peaks for the fuel phase. As for the residuum, soluble in fuel from fractional distillation, the presence of carbonyl, hydroxyl,

ester and acid functional groups is indicated. The presence of ester groups was further confirmed by NMR and mass spectrometry. For jet fuel samples, the residuum was analyzed by IR, high performance liquid chromatography (HPLC), gas chromatography/mass spectrometry (GC/MS), and gel permeation chromatography (GPC). Two conclusions were reached from the infrared spectra. First, the aromatic compounds are more concentrated in the deposit than in the fuel. Secondly, the oxygen in the residuum is attributed to carbonyl compounds; no hydroxyl groups were observed. By HPLC analyses, the residuum seemed to be high in aliphatics after the oxygen containing groups were removed. In other words, the residuum seems to be primarily aliphatic in character. GC/MS did not give much useful information. Hence, it was interpreted that the residuum contains long-chain carbonyl compounds. The average molecular weight, obtained from GPC data, is around 254.

More recently, Mayo and his colleagues used field ionization mass spectrometry (FIMS) to analyze jet fuel deposits and the oxidation products from n-dodecane.(4) They found oxidation of fuel hydrocarbons and the formation of the precursors, eg. monomers, to be the main reactions in fuel which is thermally stressed in air. The monomer precursors then proceed through condensation reac-

tions to form dimers and trimers. The decreasing of concentration of the dimers and trimers during the later stage of oxidation indicates the separation of the condensation products from fuel. It is also found that deposit precipitation is related to the increase in concentration of the polar compounds in the solution. However, the chemical structure of fuel deposits and the mechanism of their formation are still unknown despite all the useful information provided by FIMS. The investigation of the oxidation of n-dodecane, with FIMS, did not reveal much structural information on the oxidation products because the fragmentation peaks of the alcohols and hydroperoxides overlap ketone peaks. However, Mayo concluded that gum formation in fuel is affected by the species such as mono- and bi-cyclic naphthenes, alkylbenzenes, unsaturated compounds, and nitrogen and sulfur compounds (4).

Taylor and his group at Exxon have developed a model system, 2,5-DMP (2,5-dimethyl pyrrole), to study the stability of oil-shale-derived fuel. DMP was oxidized in decane at 43°C (110°F) and the solid precepitated from the liquid phase was analyzed by infrared and carbon-13 nuclear magnetic resonance spectroscopy (C-13 NMR) (16). DMP was chosen because it has been shown to be a most harmful material in shale liquid stability (16). The

conclusions of their research are listed below,

- a. Oxygen is required for sediment (deposit) formation.
- b. One or more types of carbonyl functions appear in the sediment. Ether linkages are also a possibility.
- c. The DMP sediments consist of the repeating units of partially oxidized nitrogen compounds.
- d. Sedimentation appears to be a free radical autoxidation reaction or an oxidative condensation reaction of nitrogen compounds.
- e. Sediment is not a simple type of compound but a combination of several different types of compounds.

Jones and Hazlett at Naval Research Laboratory have done C-13 NMR, Electron Spectroscopy for Chemical Analysis (ESCA), and Fourier Transform Infrared (FT-IR) analyses on the deposit produced from Shale II - derived JP-5 fuel. The fuel was spiked with 2,5-dimethyl pyrrole (500 ppm N content) and deteriorated for 25 days, at 80°C (17). According to the Cross Polarization/Magic Angle Spinning C-13 NMR (CP/MAS C-13 NMR) spectra, the oxygen in the deposit is in the form of carboxylate, carbonyl and ether linkages. ESCA and FT-IR data show the oxygen is incorporated in more than one species in the deposit.

Worstell (14) tested a model system, tetralin and dodecane (1/10, V/V), to simulate the Jet A fuel system.

A model deposit was obtained after the model fuel was stored at 121°C for more than one week. Model and Jet A deposits are alike in appearance. The elemental analysis results in Table 1 are similar for the two deposits. Infrared spectra also show noticeable similarities between the two. They all display a strong alcohol peak at 3400  $\text{cm}^{-1}$  and an aromatic peak around 3050  $\text{cm}^{-1}$ . In the region of 900-850  $\text{cm}^{-1}$ , a weak peak is assigned to peroxide O-O stretch. Three strong carbonyl stretching peaks are identified in the 1800  $\text{cm}^{-1}$  to the 1650  $\text{cm}^{-1}$  region and the peaks around 1052  $\text{cm}^{-1}$  may be due to cyclic alcohols. The comparison of peaks for two deposits is in Table 2.

Lauer and Vogel used Surface Enhanced Raman Spectroscopy (SERS) and IR Emission Spectroscopy to investigate the tetralin and dodecane system (18). They found aromatic compounds, polynuclear aromatics in particular, are deposit formers. Oxidation was claimed to be responsible for the formation of deposit.

Intense effort has been put into research on fuel deposits but little structural information has been obtained. Due to its complexity, insolubility in various solvents, and nonvolatility, analysis of the deposit by traditional methods is difficult. However, remarkable advan-

Table 1. CHN Analyses of the Model Deposit and Jet A Deposit from the Previous Work (14)

Fuel Sample	% C	% H	% N
Jet A	69.3	5.3	0.25
Model Fuel	70.2	6.1	0.29

Table 2. MIR-IR Absorption Bands of the Model Deposit from the Previous Work (14)

Model Deposit	Jet A Deposit
3300	3400
3062	3050
2958	2960
2937 (sh)	2930
2875	2860 (d)
1765	1762 (sh)
1722	1720
1713	1711
1666	1665
1595	1594
1573	
1458 (d)	1450
1385	
1185 (d)	1179
1125 (d)	1125
1052	1050
1028	
907	905 (sh)
872	885
750 (b)	750

wave numbers in  $\text{cm}^{-1}$ , sh = shoulder  
d = double, b = broad

ces in modern instrumentation make the analyses of such complicated samples possible. Three relatively new instrumental techniques employed in this thesis research will be introduced.

### Introduction to Secondary Ion Mass Spectrometry (SIMS)

SIMS has been widely used in inorganic analyses. Its application to analyses for organic solids (19,20,21,22) is more recent. This method is particularly useful for nonvolatile and thermally-fragile molecules, including organics, biochemicals, and organometallic compounds. The solid sample is placed in the ion source of a mass spectrometer and is bombarded with a primary ion beam ( $\text{Ar}^+$ ,  $\text{O}^+$ ,  $\text{O}_2^+$ , or  $\text{Cs}^+$  are the most commonly employed ions) (23). The fragments of the sample are sputtered away from the surface and then separated by a mass analyzer. Fig. 1 displays the basic components of SIMS.

There are two modes of operation in SIMS. One is called the static mode, which has a low surface removal rate. A very high vacuum is needed to help the desorption of volatile species. The other is called dynamic mode. This requires higher primary ion current to generate more secondary ions and so it has higher surface removal rates. To take advantage of the different surface

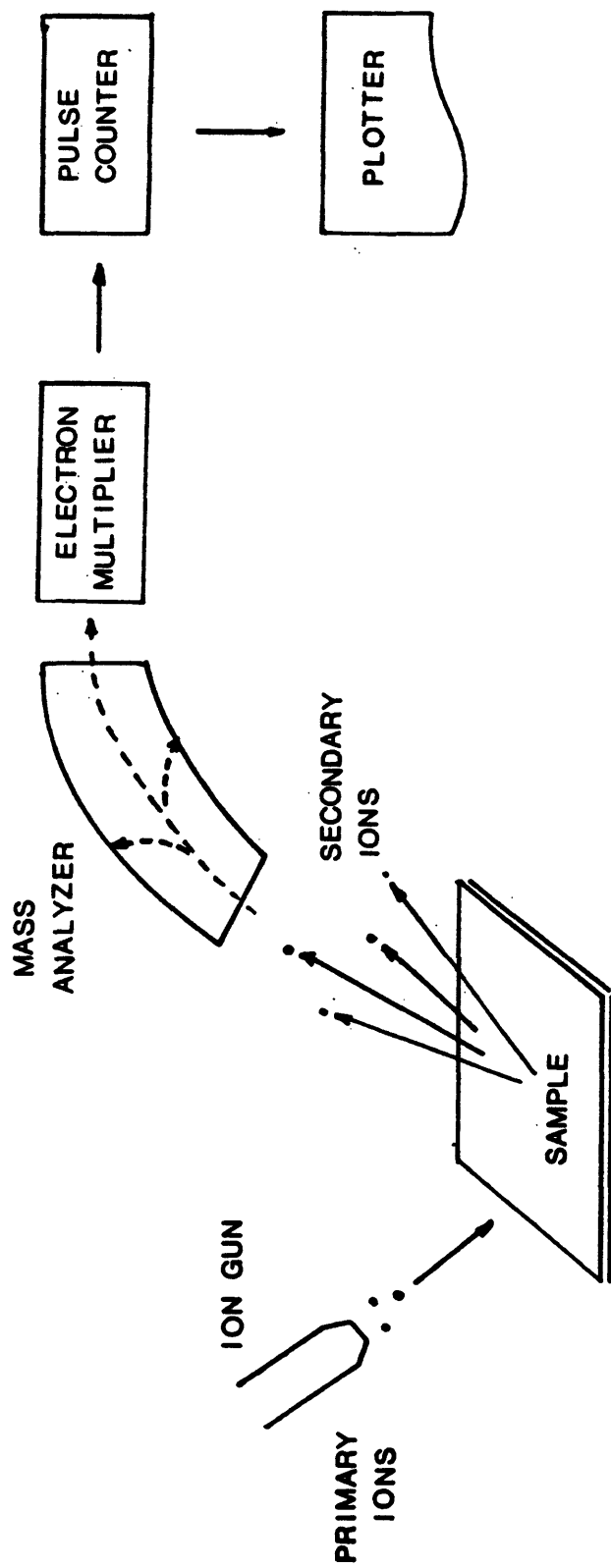


Figure 1. Basic Components of SIMS

removal rate, the static mode is usually applied to study surface species and the dynamic mode is used to study the bulk depth profile (24).

### Introduction to CP/MAS C-13 NMR

Cross Polarization (CP) C-13 NMR is one of the advanced NMR techniques developed in the 70's for analyzing solid samples. It allows the determination of the aromatic to aliphatic carbon ratio in solids. And the carbon chemical shifts provide information about the chemical structure and the functional groups (25,26,27).

In this technique, the enhancement of the C-13 signals is achieved by transferring the magnetization from protons; then, resonance is observed under proton decoupling. The process of cross polarization was originally described by Pines, Gibby and Waugh (28). A strong rf pulse (intensity  $H_{1h}$ ) at the  $H^1$  resonance frequency is applied to the sample for a sufficient time to tip the net proton magnetization vector 90 degrees from  $H_0$  (applied magnetic field). The second rf field (intensity  $H_{1c}$ ) is added at the C-13 resonance frequency and maintained for a time  $t_{cp}$  which is called "contact time". A very efficient magnetization (energy) transfer from the proton set spin to the C-13 set spin occurs under the Hamann-Hahn condition such

that  $r_H H_{1h} = r_C H_{1c}$  where  $r_H$  and  $r_C$  are the magnetogyric ratios of H1 and C-13. This process occurs much faster than C-13 spin-lattice relaxation, and the repetition of the pulse can enhance the net C-13 magnetization to raise the S/N ratio. After the contact period,  $t_p$ , the C-13 rf is turned off, while the proton rf field is still maintained for C<sup>13</sup>-H<sup>1</sup> dipolar decoupling in the data acquisition period. The time averaged free induction decay is then Fourier transformed to plot the regular C-13 NMR spectrum.

Magic Angle Spinning (MAS) is another technique used in C-13 NMR to eliminate the line broadening which is caused by dipole-dipole interactions ( $H_D$ ). In a liquid,  $H_D$  is averaged to zero because of the rapid isotropic molecular tumbling. But in a solid,  $H_D$  is not zero because molecules, confined in a rigid lattice, have no tumbling space. From the Hamiltonian of the dipolar interactions between two molecules,  $(1-3\cos^2\theta_{ij})$  can be derived as the angular dependence for  $H_D$ , where  $\theta_{ij}$  is between the applied field and the intermolecular vector (29). In this case, if the solid sample is spun at an angle (magic angle) of  $54.44^\circ$ ,  $(1-3\cos^2\theta_{ij})$  will be equal to zero and  $H$  can be reduced or eliminated. The anisotropic interaction of the chemical shift also will be erased. However, the high spinning rate of the sample, usually on the order of KHz,

necessary for removing the dipolar broadening is very difficult to achieve in the magic angle spinning procedure. By combining with the Cross Polarization technique, the line broadening problem can be greatly improved.

Schaefer and Stejskal (30) have performed natural and synthetic polymer analyses by CP/MAS C-13 NMR. They have proved this combination is a very powerful tool for solid state NMR analysis.

#### Introduction to Multiple Internal Reflectance Infrared (MIR-IR)

Attenuated Total Reflection Infrared, ATR-IR, was developed by Dr. J. Fraherenfort in the late 1950's for obtaining infrared data on dense plastic materials. This technique suffered from poor sensitivity and serious distortion of spectra. Multiple internal reflectance (MIR) was then developed and improved greatly on the spectra obtained. MIR has been successfully used to analyze both solid and liquid materials (31). Total reflectance occurs when the incident angle of the light beam is greater than or equal to the critical angle and the radiation is traveling from a more dense to a less dense medium. The critical angle  $\theta_c$  is defined as  $\text{Sin } \theta_c = N_2/N_1$ , where the radiation passes from the medium with refraction index  $N_1$  to

that with index of refraction  $N_2$ . This phenomenon is depicted in Fig. 2(a). If the light beam is viewed as waves, the beam penetrates the prism surface where total reflectance occurs. By applying infrared as the light source and coating the sample on the prism surface, infrared absorption occurs due to the infrared radiation traveling through the sample phase as total reflectance occurs.

Multiple internal reflectance is made possible by a well-polished trapezoidal plate which is made of certain inorganic materials of appropriate refractive index and transparency range. As shown in Fig. 2(b), the IR beam enters the plate from the angled-face on the right and is reflected from one of the parallel faces, both coated with sample, to the other until it exits from the angled face on the left. The IR absorption is greatly enhanced this way and the beam incident angle need not be brought close to the critical angle to decrease the distortion. The depth of beam penetration is on the order of the beam wavelength. For instance, a  $45^\circ$  angle-of-incidence, KRS-5 plate, with refractive index 2.4, allows the IR beam to penetrate about one wavelength. The consistency of penetration adds one more advantage to the MIR technique. That is the thickness of sample layer does not affect

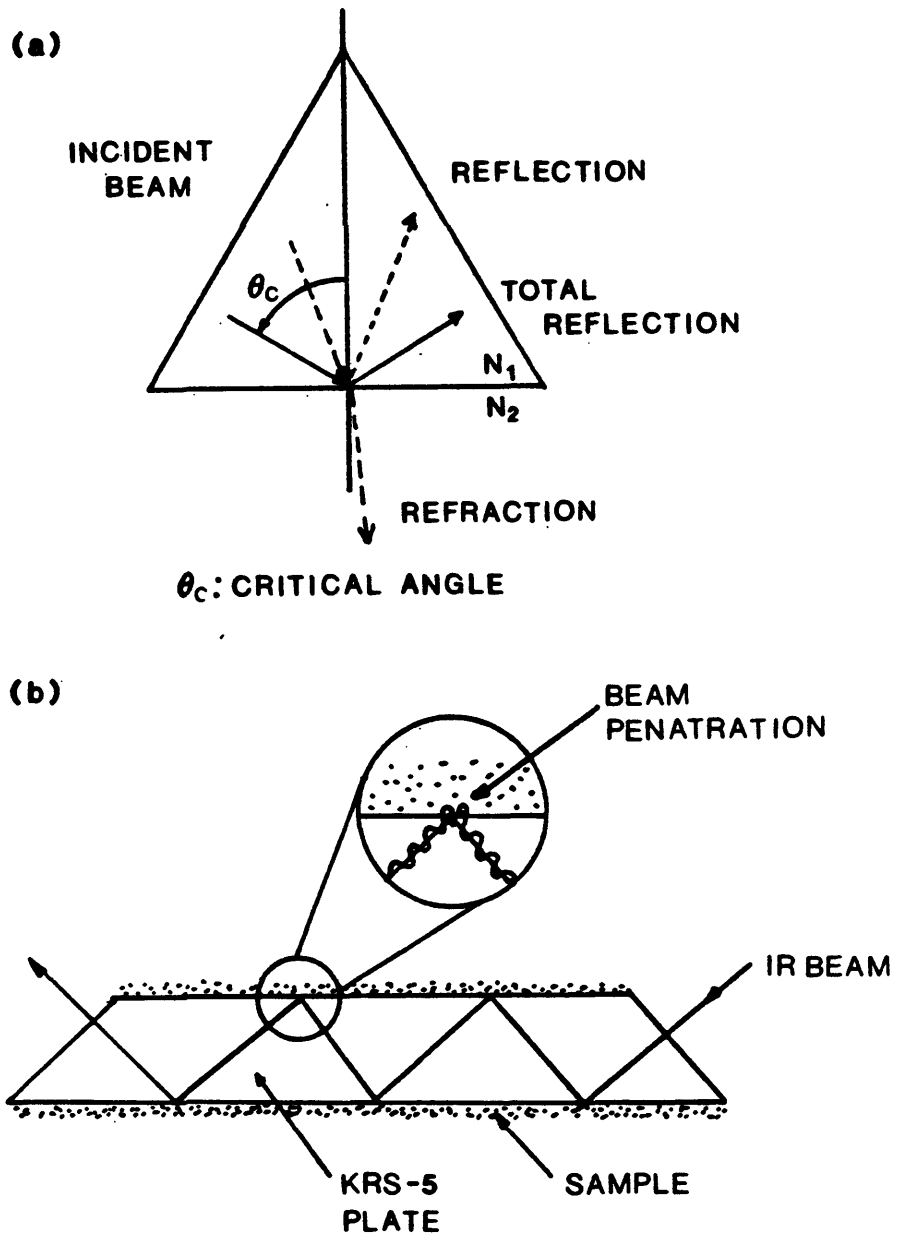


Figure 2. (a) Total Reflectance  
 (b) Multiple Internal Reflectance

spectrum intensity as long as it is thicker than several wavelengths. MIR provides a solution to obtaining an IR spectrum on a solid sample with poor solubility. The thickness control problem of viscous liquid samples and tedious sample preparation is avoided.

## EXPERIMENTAL WORK

Preparation of Chemicals and Reagents

Jet A fuel was acquired from the National Aeronautics and Space Administration (NASA) Lewis Research Center. It was stored at 4°C and then filtered through a fine sintered-glass funnel prior to use. Technical grade n-dodecane was purchased from the J.T. Baker Chemical Co., Phillipsburg, NJ; 99% pure n-dodecane was purchased from Aldrich Chemical Co., Milwaukee, WI. Since unsaturated species are reactive, it is necessary to remove them from the n-dodecane. Both batches of dodecane were first washed with concentrated sulfuric acid until the acid layer was colorless, indicating that all unsaturated compounds had been removed. The acid-washed dodecane was then washed several times with 5% aqueous sodium bicarbonate solution. The neutralized dodecane was then washed twice with demineralized water and distilled. The purity of dodecane was checked to be above 95% by GC. To be sure that no unsaturated compounds remained, purified n-dodecane was analyzed by HPLC using UV detector (254 nm) which has low detection limits for unsaturates. As for the GC method, the peak area of the n-dodecane is, by assuming equal response factor, divided by the total peak area to

obtain the percentage purity for n-dodecane. Technical grade tetralin was purchased from J.T. Baker Chemical Co., Phillipsburg, NJ. The tetralin was treated with activated silica gel and distilled. The distilled tetralin was collected from 197 to 199°C and again passed through a column of activated silica gel to remove any peroxides or their decomposition products. The purity was checked by GC and HPLC.

Activated silica gel, 60-200 mesh, was purchased from two companies, Eagle Chemical Co., Mobile, AL and Davison Chemical, Baltimore, ML. Although the silica gel was labeled "activated", it was always reactivated in a 400°C oven for 24 hours prior to use.

High Performance Liquid Chromatography (HPLC) grade hexane, isooctane, tetrahydrofuran (THF), and chloroform were purchased from Fisher Scientific Company, Fair Lawn, NJ. Chloroform was passed through activated silica gel to remove the small amount of ethanol which functions as a stabilizer. Hexane, isooctane, and THF were used as received. All the solvents were distilled for reuse. In the THF distillation, ferrous sulfate was added to the pot to prevent the potential hazard caused by peroxides. The distilled THF was then passed through activated alumina to remove any residual peroxides. It was then stored in a

glass bottle under refrigeration.

Deuterated chloroform was obtained from Norell Chemical Co., Inc., Landisville, NJ. Acetonitrile was purchased from Burdick & Jackson Laboratories Inc. Muskegon, Mich. 1-Tetralone was obtained from Aldrich Chemical Company Inc., Milwaukee, WI. Reagent grade dichloromethane and semicarbazide hydrochloride were obtained from Matheson Coleman & Bell, Cincinnati, OH. Potassium dichromate and hydroxylamine hydrochloride were purchased from Allied Chemical, Morristown, NJ. Acetone was purchased from J.T. Baker Chemical Co., Phillipsburg, NJ. Methanol was obtained from Eastman Kodak Company, Rochester, NY. Sulfuric acid was purchased from Manufacturing Chemists Inc., Cincinnati, OH. Sodium acetate was purchased from Mallinckrodt Chemical Works, St. Louis, MO.

#### Instrumental Analyses

A Varian Model 3700 Gas Chromatograph equipped with a Flame Ionization Detector (FID), column (2m x 1/8 in. SS) packed with 3% OV-17 on Chrom W-H.P. (80/100) was used to check the purity of tetralin and dodecane. The temperature was set at 180°C for one minute and then programmed at the rate of 10°C/min. to 230°C. The final temperature, 230°C, was maintained for five minutes. The oven was then

cooled to the initial condition for the next run. The temperatures of the injector and detector were fixed at 230°C.

A Waters Associates HPLC equipped with a U6K Sample injector, a model 440 UV Detector ( $\lambda=254\text{nm}$ ), a model R401 Refractometer (as a second detector), and two Hewlett Packard (HP) 3390 Integrators (for plotting peaks and integrating peak areas) were used. A Waters Associates  $\mu$ -Porasil column was used for normal-phase separation. A Waters Associates Ultra-Styrigel 100 A column was used for gel permeation chromatography (GPC). Polystyrene and aromatic hydrocarbons, from Waters Associates, were used as standards for the molecular weight calibration. For all HPLC experiments, the flow rate was constant at 2 ml/min. For all experiments, the attenuator of the refractive index detector was set at 8X and the sensitivity unit of the UV detector was set at 2.0.

All PNMR analyses were performed on a Varian EM 360A Nuclear Magnetic Resonance Spectrometer (60 Hz). Samples were analyzed in 5 mm, thin wall sample tubes.

A Perkin-Elmer 521 Double-Beam Grating Infrared Spectrophotometer and Wilks 9 Multiple Internal Reflection attachment were used to perform the Multiple Internal Reflectance Infrared (MIR-IR) analyses. The instrumental

operating parameters were set as follows: Scan Time, 32; Suppression, 4; Expansion, 1X; Attenuation Speed, 1.5 to 6; Resolution, 6.5; Slit Program, 10; and Source Current, 0.8.

The capillary GC work was done in the Department of Chemical and Petroleum Refining Engineering of CSM using an HP5840 Gas Chromatograph. The capillary column was a 15 m X 0.25 mm DB-5 bonded phase column from J and W Scientific Inc., Rancho Cordova, CA. It was operated under the following conditions: Initial Temperature, 75°C; Final Temperature, 250°C; Injector Temperature, 300°C; Detector Temperature, 350°C; Attenuation, 4; and He Flow Rate, 30 ml/min. The temperature was programmed to remain at 75°C for two minutes, then to increase at a rate of 2.5 °C/min. for three minutes, increase to a rate of 15°C/min. for eight minutes, and then increase at 5°C/min. until the final temperature, 250°C, was reached. The program was completed after the final temperature was held for five minute. The oven was then cooled to the initial temperature for another run. Split ratio was set at 100 to 1 at 1 ml/min flow rate.

An Extranuclear Quadrupole Mass Spectrometer, equipped with a sample pyrolysis device (PY-MS), was used to obtain pyrolysis mass spectra of the deposits. The run-

ning conditions were: wire equilibrium temperature, 510°C; scanning rate, 0.236 s/scan; total scanning time, 7.08 s; and electron voltage, 15.0 eV. The spectra were scanned from m/e of 33 to 400. All the PY/MS experiments were performed by Dr. R. Tsao at the Department of Chemistry & Geochemistry at the Colorado School of Mines, Golden, CO.

A Carlo-Erba 1104 Elemental Analyzer was used to analyze the carbon (C), hydrogen (H), and nitrogen (N) content of the deposits. The oxygen content was calculated by subtracting the C, H, N content from 100%.

GC/MS analyses were performed on a GC/MS/DS system made by Extranuclear Laboratories Inc.

#### Other Analyses

The CP/MAS Carbon-13 NMR analyses were performed by the Colorado State University Regional NMR Center, Fort Collins, CO. Liquid C-13 NMR analyses were conducted at the Solar Energy Research Institute by Dr. Marvin Curtis. SIMS analyses were done by Dr. Robert Orth at the Department of Chemistry, University of Utah, Salt Lake City, UT.

#### The Preparation of the Jet A Deposit and the Model Deposit

Deposits from both Jet A fuel and a model fuel (tetralin/dodecane, 1/10, V/V) were analyzed.

The Jet A deposit was acquired from Dr. Jonathan Worstell who was previously a graduate student in the Department of Chemistry & Geochemistry at the Colorado School of Mines. It had been produced by aging Jet A fuel at 121°C for 168 hours, collecting the solid phase, and washing it with hexane (14). The model deposit was obtained by mixing 20 ml of tetralin with 200 ml of dodecane in a 500 ml three-necked round-bottom flask. The reaction temperature was maintained at 120±5°C for 168 hours, while air was bubbled through the liquid phase. A dark brown gummy solid was formed. It was then separated from the model fuel and was washed several times with hexane/petroleum ether. The resulting solid is powdery and its color is a lighter brown than that of the original gummy solid.

#### Physical Properties of the Deposits

Solubility of model deposits in different solvents was tested by adding model deposit to one milliliter of dichloromethane, chloroform, dimethylsulfide, or THF until undissolved solid settled to the bottom of vials. The vials were capped and allowed to stand overnight. Each mixture was then filtered through a millipore filter (0.5 um) and the solution was evaporated to dryness at room

temperature and recovered solid was weighed. The melting points of Jet A deposit and model deposit were measured using a Thomas Hoover Capillary Melting Point apparatus.

Both Jet A deposit and the model deposit were sent to the Chemical and Petroleum Refining Department for elemental analysis. An empirical formula for each deposit was calculated from the carbon, hydrogen, nitrogen, and oxygen contents in the deposits thus obtained.

#### The Variation of Aliphatic Hydrogen and Aromatic Hydrogen Ratio in Aged Model Fuel

Ten milliliters of model fuel (tetralin/dodecane, 1/10, V/V) were pipeted into a soft glass bottle with a cap lined with PTFE sheet. The sample was aged at 121°C for seven days. Samples were withdrawn from the bottle and analyzed by PNMR every 24 hours. The areas of peaks were integrated in two regions. The total peak area between 6 ppm and 8 ppm was assigned to aromatic hydrogen. The total peak area between 2 ppm and 4 ppm was attributed to aliphatic hydrogen. The ratios were then calculated and compared.

#### Dichloromethane and THF Extracts of Deposits

The model deposit and Jet A deposit were added into

dichloromethane and filtered through a Millipore filtering device (0.45 micron). The filtrate was saved as dichloromethane extract. The microfilters containing dichloromethane-insoluble components were put into THF and shaken vigorously. THF mixtures were filtered using the same procedure and the filtrate was collected as THF extract. The dichloromethane and the THF extracts for both deposits were analyzed by HPLC and PY/MS. For the HPLC analyses of dichloromethane extracts, a mixture of 80% isooctane and 20% chloroform with a small amount of acetonitrile added was used as the mobile phase. The mobile phase for THF extracts was programmed through a linear path from complete 80% isooctane 20% chloroform to pure THF. For the PY/MS analysis, the different extracts were coated on ferromagnetic wires using a syringe. Then, the solvent was evaporated using a warm air blower. Data acquisition, plotting of spectra, and data manipulation were performed using a PDP-11/10 minicomputer.

#### The Separation and Collection of the Components in the Dichloromethane Extract of the Model Deposit

Various compositions of a hexane/chloroform mixture were tested as an HPLC elution solvent for obtaining good separation of the different species in the dichloromethane

extract of model deposit. A reasonably good separation is achieved with the elution solvent consisting of 80% hexane/20% chloroform. Hexane was chosen because of its volatility which allows solvent to be quickly removed from the components collected.

It was necessary to know the dead volume between the UV detector and the outlet for sample collection, which was measured by running methylene blue aqueous ethanol solution (1g of methylene blue in 25 ml water and 65 ml ethanol) through the HPLC. Nineteen seconds were measured for the time elapsed between the peak showing up on the integrator for UV detection and the observation of the blue drop at the outlet. The dead volume, 0.63 ml, was then calculated from the flow rate of 2 ml/min. Sample collection was achieved by opening the collection valve nineteen seconds after the peak of the desired component just appeared on the integrator, and shutting the valve thirty seconds after the peak starts to tail. Five fractions were collected. In order to obtain enough material for instrumental analysis, the above procedure was repeated several times and the HPLC eluent (solvent) was evaporated at room temperature. Those fractions were analyzed by MIR-IR, capillary GC, and PY/MS.

### Benzene and THF Extracts of Deposits

In this experiment, the same procedures as described the previous section, dichloromethane and THF extracts of deposits, were applied with the exception that benzene was used in lieu of dichloromethane. These extracts were analyzed by MIR-IR, HPLC, and PY/MS.

### Group Separation by Open Column Chromatography of Model Deposit

Due to the limited amount of the Jet A deposit, this separation was applied only to the model deposit. The purpose of this method is to separate the model deposit into several fractions by Bond Elute column chromatography with cyanopropyl (CN) modified and unbonded silica gel (SI) column packing. These columns were purchased from Analytichem International Inc., Harbor City, CA. The Bond Elute column has the advantage over the conventional silica/alumina column packing for chromatographic separation in its simplicity and reproducibility (32).

Model deposit was placed on top of the CN column which was connected on top of the SI column with an adapter. The columns were conditioned with 6 ml of hexane first, then followed by a series of solvent elutions. Six milliliters of benzene were passed through the columns to

elute the aromatic fraction. After that, two columns were taken apart and each was eluted with 4 ml of benzene/chloroform mixture (3/1, V/V) to obtain the aromatics with moderate polarity. The CN column was then eluted with 6 ml of chloroform to collect the polar fraction. The last fraction, compounds with high polarity, was obtained by passing 6 ml of methanol through the CN column. Each fraction was dried under nitrogen gas and analyzed by GC/MS.

#### Sample Preparation for SIMS Analysis

A thermal deposit was acquired from the NASA Lewis Research Center. This deposit was prepared in a simulator on aluminum foil at 260°C while 700 ml of Jet A fuel flowed over the aluminum foil surface. The temperature of the surface was raised from ambient to 260°C in 0.5 hour; maintained at 260°C for 2.5 hours; and then cooled to ambient temperature in 0.5 hour.

The samples of Jet A deposit and the model deposit were prepared by slurring the deposit in THF, coating on a 18 mm X 18 mm coverslip, and air-drying the coverslips.

#### Sample Preparation for Carbon-13 NMR Analysis

For CP/MAS C-13 NMR analysis, 0.8711 g of model

deposit and 0.3646 g of Jet A deposit were mailed to Colorado State University Regional NMR Center without any treatment.

Another set of samples was prepared for C-13 NMR analysis (solution phase) at SERI. The model deposit was dissolved in deuterated chloroform (concentration of 15% by weight). A saturated deuterated chloroform solution of Jet A deposit was also made. Both solutions were filtered through a 0.5 m Millipore filtering device to remove the suspended particles. PNMR analysis was also performed on both samples.

#### Wet Chemical Analysis

Traditional laboratory organic functional group identification techniques (33) were employed to help distinguish aldehydes from ketones. Five tests were conducted on the model deposit including: the 2,4-dinitrophenylhydrazine test for identifying the carbonyl group in aldehydes and ketones; Benedict's solution test; Tollens' reagent test, and the fuchsin-aldehyde reagent test. The chromic anhydride test was used to identify alcohol groups. The model deposit was dissolved in dioxane for all tests requiring liquid sample.

### Derivatives of 1-Tetralone and the Model Deposit

1-Tetralone has been suspected to be the precursor of deposits (14). Therefore, oxime and semicarbazone derivatives of the model deposit and tetralone were prepared by the standard procedures.(34)

### Detecting Peroxide Linkage in the Model Deposit

The autoxidation of tetralin has been thought to be the initial step of deposit formation (14). The possibility of condensation reactions between the hydroperoxide and tetralone was examined by attempting to detect peroxide bonds in the deposit. The model deposit was partially dissolved in tetralin because tetralin releases the  $\alpha$ -hydrogen easily; therefore peroxide bond homolysis should lead to -OH formation via H abstraction from tetralin. The mixture was kept at 200°C in a three-necked round-bottom flask. A magnetic stirrer was used to minimize temperature gradients. A condenser was added to retain tetralin in the system. The whole system was maintained under nitrogen atmosphere to prevent the oxidation of tetralin. A small amount of the liquid phase was withdrawn every 24 hours and analyzed by MIR-IR. If peroxide bond existed, an increasing OH absorption should be observed in IR spectra.

## RESULTS AND DISCUSSION

This section is divided into several subsections corresponding to the various experiments performed.

### Gel Permeation Chromatography (GPC)

In this study the molecular weight of the Jet A deposit and the model deposit are found to be 1000 and 400 respectively. These results were obtained based on polystyrene calibration standard.

### High Performance Liquid Chromatography (HPLC)

As shown in Fig. 3, there are several peaks in the chromatogram of the model deposit and the Jet A deposit. That indicates each of the two deposits consists of more than one component.

### Carbon, Hydrogen, and Nitrogen Analyses

CHN analyses of the model deposit and Jet A deposit are very similiar. The model deposit does not, however, contain nitrogen because the reactants, tetralin and dodecane, of the model system do not contain nitrogen.

The weight percent of carbon, hydrogen, nitrogen,

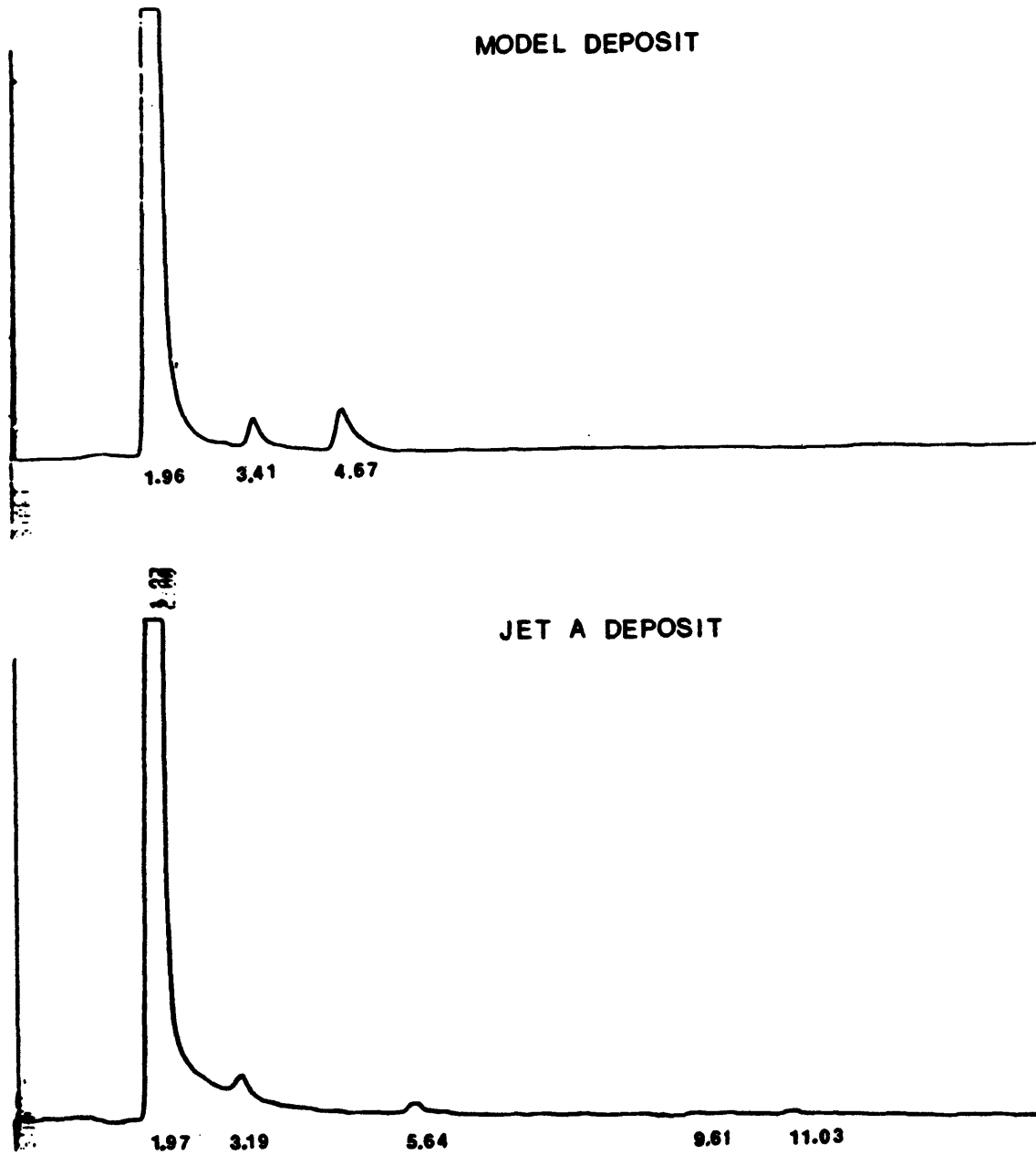


Figure 3. HPLC Separation of the Model Deposit and the Jet A Deposit

oxygen, and the hydrogen to carbon ratio are listed in Table 3. This table also includes the calculated data, for the items described above, for several possible oxidation products of tetralone (35). The calculated carbon, hydrogen, nitrogen and oxygen contents of tetralone show higher values of carbon and hydrogen but a lower value of oxygen compared to those of the model deposit and the Jet A deposit. However, 1,4-dihydroxy-naphthalene, 1,4-naphthoquinone, and 4-hydroxy-1,2,3,4-tetrahydronaphthalenone have compositions near that found for the deposits. This result agrees with an experiment performed by Dr. S. R. Daniel's group at Colorado School of Mines. In the experiment, tetralone was dissolved in n-dodecane and sealed in vials which were filled with carbon dioxide. Those vials were aged at 121°C for over a week. No deposit formed and the color of the solution did not change significantly. However, the deposit formed rapidly after air was introduced into the system. It was concluded that tetralone itself may not be responsible for deposit formation but its oxidation products are (36).

Both deposits have H/C ratio less than one, which indicates more unsaturated carbons or functional groups in the deposits than present in tetralone. The H/C ratio of the model deposit is close to that of indanone; the H/C

Table 3. Carbon, Hydrogen, and Nitrogen Analysis for the Model Deposit and the Jet A Deposit

	Carbon%	Hydrogen%	Nitrogen%	Oxygen%
Jet A Deposit (a)	73.34	5.59	0.22	21.85
	74.03	5.79	0.22	19.96
	73.68	5.69	0.22	20.41
average (b)	73.68±0.85	5.69±0.25	0.22	20.74
Model Deposit (a)	72.59	5.56	0	21.85
	72.79	5.63	0	21.58
	72.10	5.52	0	22.38
average (b)	72.49±0.88	5.57±0.14	0	21.94
Tetralone (c)	82.19	6.85	----	10.90
Indanone (c)	81.82	6.06	----	12.12
Tetralol (c)	81.08	8.11	----	10.81
Napthoquinone (c)	75.95	7.59	----	20.25
1,4-dihydroxy-naphthalene (c)	74.07	6.11	----	19.75

(a) : experimental data

(b) : 95% confidence interval with normal distribution

(c) : calculated from chemical formula

ratio of the Jet A deposit is close to that of 1,4-dihydroxynaphthalene.

#### Derivatives of 1-Tetralone and Model deposit

An attempt was made to obtain the melting point of the model deposit as well as the Jet A deposit; however, there was no significant phase change up to the maximum temperature limit of the equipment which is 320°C. Table 4 shows the measured melting points of the oxime and the semicarbazone derivatives of the model deposit as well as of tetralone. The oxime of the model deposit has a melting point of 150°C-152°C and its semicarbazone derivative has a wider range, 245°C-250°C. The same derivatives with tetralone yielded significantly different melting points: oxime 102°C and semicarbazone 220°C-225°C. The values for the model deposit are close to literature values (37) for 1,2- and 1,4-naphthoquinone as shown on the last two rows in Table 4. These results reinforce the conclusions from CHN analyses that oxidation products of tetralone are model deposit precursors.

#### Functional Group Investigation by Wet Chemical Techniques

The presence of aldehydes or ketone carbonyl in the the model deposit was investigated by wet chemical methods.

Table 4. The Melting Point of Model Deposit and Tetralone Derivatives

	Oxime Deriv.	Semicarbazone Deriv.
Model Deposit (a)	150 - 152°C	245-250°C
1-Tetralone (a)	102 - 103°C	220-225°C
1-Tetralone (b)	102°C	217°C
1,2-Naphthoquinone (b)	162-164°C	184°C (d)
1,4-Naphthoquinone (b)	-----	247°C

(a): experimental data

(b): melting points of both derivatives are obtained from the CRC Handbook, 58th ed.

(d): decomposed

Table 5. Summary of Wet Chemical Analyses

Type of test	Purpose	Results
Chromic Anhydride	detect -OH groups	opaque greenish blue solution (+)
2,4-Dinitrophenyl-hydrazine	detect carbonyl groups	orange precipitate (+)
Benedict's Solution	detect aldehyde groups	trace amount of red ppt. (-)
Fuchsin-Aldehyde Reagent	detect aldehyde groups	light purple color (-)
Tollen's Reagent	detect aldehyde groups and certain phenols	no silver mirror developed (-)

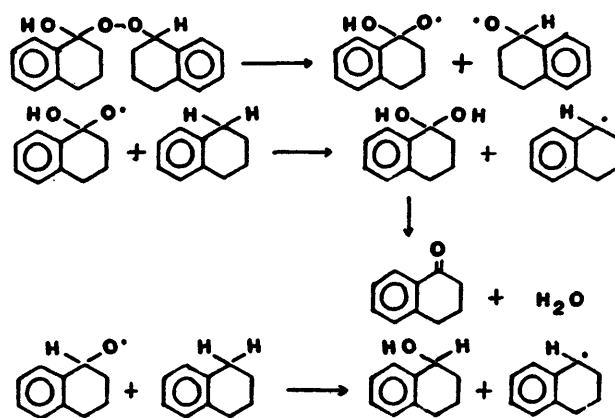
-----

(+): positive response  
 (-): negative response

Experimental results are listed in Table 5. As the results show, the carbonyl group in the model deposit is ketonic. And the alcohol group is likely to be in the model deposit.

The Test of the Peroxy Linkage in the Model Deposit

Worstell (14) has suggested that the model deposit is caused by a condensation reaction between tetralin hydroperoxides and tetralone to form a peroxy bridge. If that is true, as shown below, the peroxy bridge should undergo thermal homolytic cleavage and, in the presence of tetralin, abstract an H atom to generate an alcohol.



The intensity of the OH band in the infrared region should increase as the reaction proceeds. No significant difference of OH absorption intensity was observed on the samples withdrawn from the reaction vessel during the

reaction time period. This suggests that the peroxy linkage does not exist in the model deposit and that the condensation reaction of tetralin hydroperoxide with tetralone is not responsible for the deposit formation. Or that the alcohols produced were not soluble in the liquid phase. However, the nature of broad OH absorption makes quantification of the intensity imprecise.

#### MIR-IR Analyses of Model Deposit and Jet A Deposit

In these analyses, model deposit and Jet A deposit show many similarities (Fig. 4). They each have a broad OH peak around  $3300\text{ cm}^{-1}$  to  $3400\text{ cm}^{-1}$ . In the aromatic C-H stretching region, Jet A deposit does not show a resolved peak as model deposit does. But those CH absorptions of the Jet A deposit may be buried in the broad OH band. The peaks between  $1400\text{ cm}^{-1}$  and  $1600\text{ cm}^{-1}$  are assigned to aromatic hydrogen for both deposits. The aliphatic C-H stretching region is well defined in the spectra of the model deposit and the Jet A deposit by the peaks at  $2920\text{ cm}^{-1}$  and  $2850\text{ cm}^{-1}$ . Carbonyl peaks, around  $1700\text{ cm}^{-1}$ , in both spectra are interpreted as ketone or acid. Aldehyde is excluded due to absence of peaks at  $2710\text{ cm}^{-1}$  characteristic of the aldehyde hydrogen. The broad band around  $1200\text{ cm}^{-1}$  in both spectra may represent several overlapping

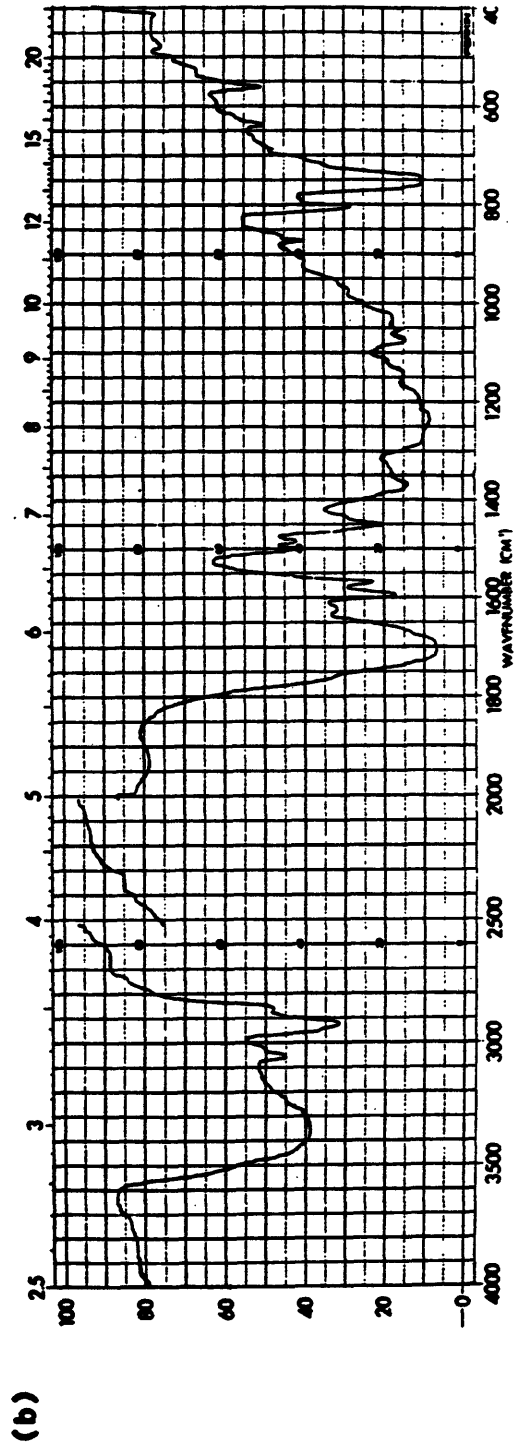
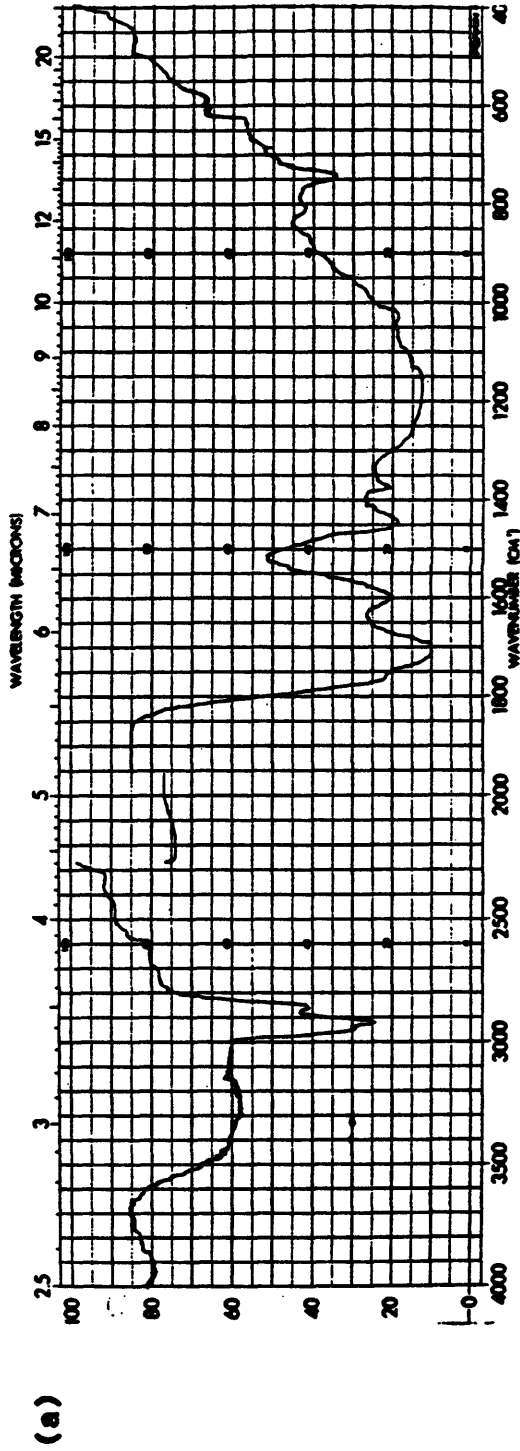


Figure 4. MIR-IR Spectra of (a) Jet A Deposit (b) Model Deposit

peaks. The double peaks at  $750\text{ cm}^{-1}$  and  $800\text{ cm}^{-1}$  have been assigned to peroxy linkage according to previous work (14). The small peak at  $1625\text{ cm}^{-1}$  in the spectrum of model deposit is due to C=C.

The Comparison of MIR-IR Analyses of the Benzene Extract and the Benzene-insoluble/THF-soluble Fraction of the Model Deposit

In this section, "THF fraction" refers to the fraction of the model deposit which is benzene-insoluble but THF-soluble.

Some aromatic compounds are expected to be soluble in benzene. In the benzene-soluble fraction, an alcohol band occurs at  $3400\text{ cm}^{-1}$ , aromatic C-H stretching at  $3050\text{ cm}^{-1}$ , and aliphatic C-H stretching around  $2850\text{--}2990\text{ cm}^{-1}$  (Fig. 5). Absorptions around  $1595\text{ cm}^{-1}$ ,  $1575\text{ cm}^{-1}$ , and  $1480\text{ cm}^{-1}$  further indicate aromatic compounds. Condensed ring systems can also contribute to the absorption at  $1595\text{ cm}^{-1}$ . Weak shoulder peaks in the  $840\text{ cm}^{-1}$  to  $900\text{ cm}^{-1}$  area are assigned to peroxy linkages.

Compared to benzene extract, the THF fraction of the model deposit has much lower overall intensity throughout the spectrum. The absorption intensity of MIR-IR varies with the wavelength of the IR beam. Nevertheless, with

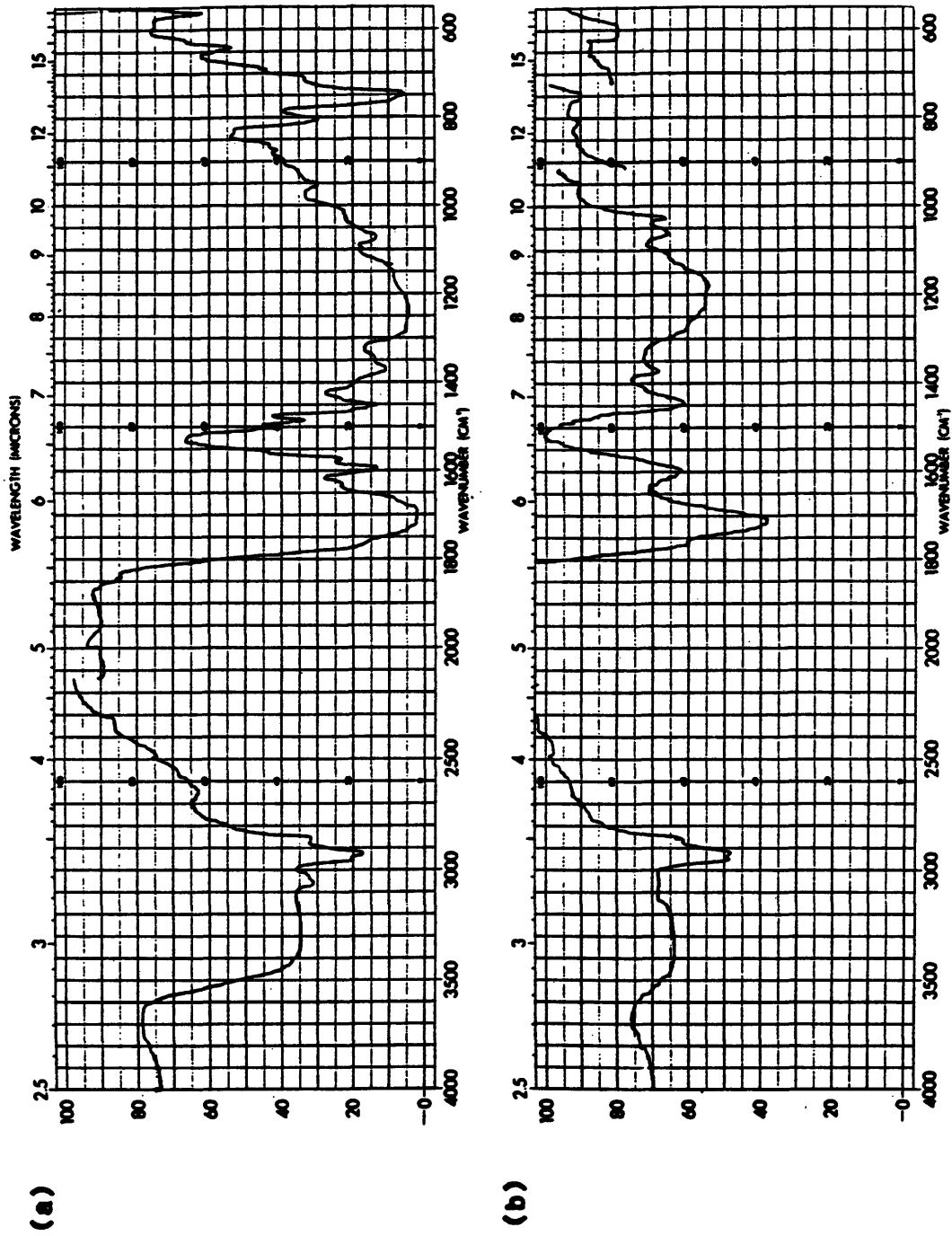


Figure 5. MIR-IR Spectra of the Model Deposit  
(a) Benzene Extract (b) THF Fraction

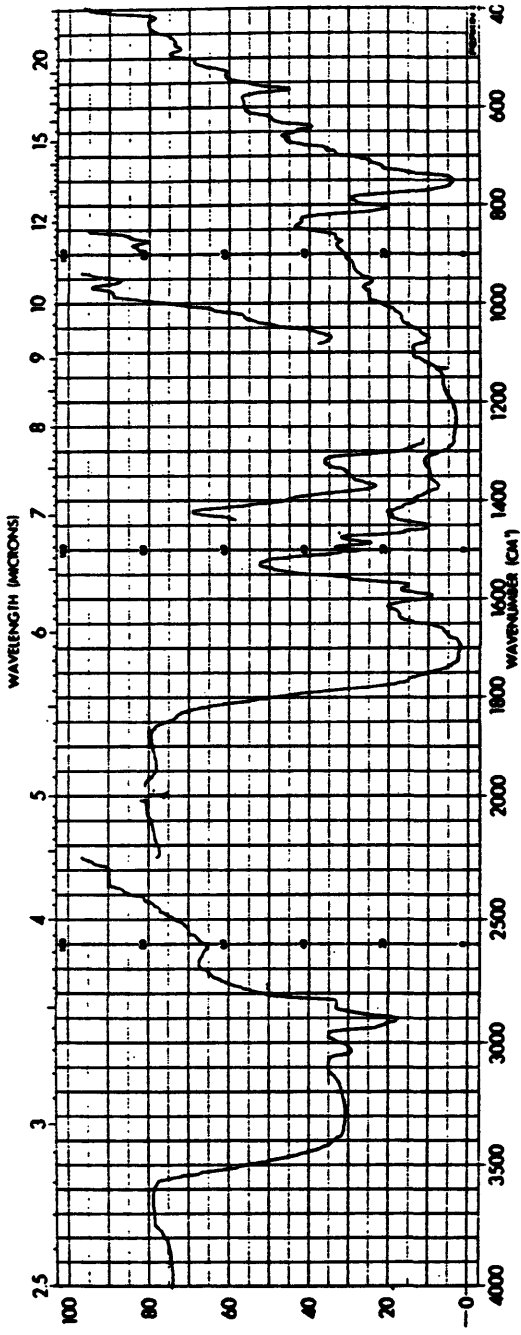
the same attenuator setting, the peak intensity at the same wavelength could be compared in accordance to the appearance of the peak by assuming the variance is the same at the same wavelength. As described in the "Introduction", the depth of the penetration of IR beam and the number of reflectances are constants if the same plate is used throughout the experiment. That rules out the intensity variation as due to uneven sample coating. So the intensities of MIR-IR in this study are based on the quantity of each functional group in the sample. The intensity of OH band is greatly reduced and the aromatic C-H stretching peak disappeared as expected. The decreased intensity of the saturated C-H stretching indicates the benzene-soluble fraction contains saturated C-H bonds. The carbonyl group has broad peaks in the 1650-1700  $\text{cm}^{-1}$  region as shown in the spectrum of the benzene-soluble fraction. But in the same region for the THF fraction, the peak intensity is reduced substantially. This indicates that the carbonyl groups are with the aromatic ring system. Around 1480  $\text{cm}^{-1}$ , a C=C stretching is shown in the spectrum of the benzene extract but not in the THF fraction. Peaks around 1050  $\text{cm}^{-1}$  are attributed to the ring vibration of cyclic compounds which is not seen in the spectrum of the benzene extract.

The following conclusions can be drawn from the above comparisons; an aromatic ring system is the backbone of the compounds in the model deposit. They contain the carbonyl group, hydroxyl group, and acidic group or peroxy linkage.

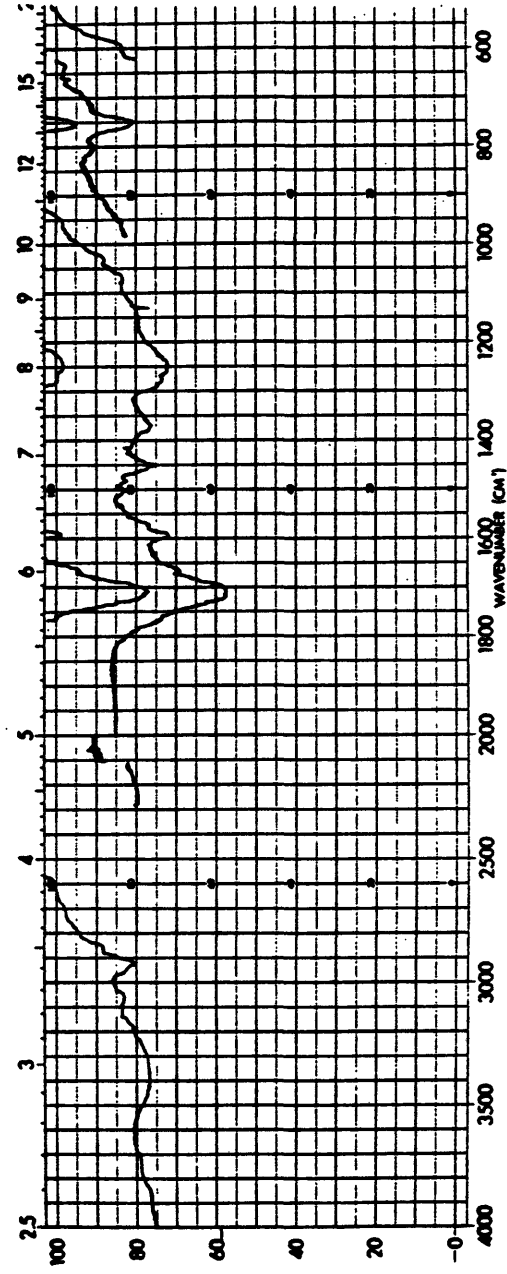
The Comparison of MIR-IR Analyses of the Dichloromethane Extract and the Dichloromethane-insoluble/THF-soluble Fraction of the Model Deposit

In this section, "THF fraction" refers to the fraction of the model deposit which is dichloromethane-insoluble but THF-soluble.

The IR spectrum of dichloromethane extract is almost identical to that of the model deposit (solid) and that of the benzene extract. (Fig. 6 and Fig. 5) Some minor differences are distinguished around  $2600\text{ cm}^{-1}$  and  $1150\text{ cm}^{-1}$ . The comparison of the dichloromethane soluble and THF fraction is obvious; most of the materials in the model deposit are soluble in dichloromethane. From the above result, most of the compounds in the model deposit have moderate polarity. Only a small fraction of the material is composed of components of higher polarity. And the dichloromethane-soluble fraction contains mostly aromatic compounds.



(a)



(b)

Figure 6. MIR-IR Spectra of the Model Deposit  
(a) Dichloromethane Extract (b) THF Fraction

Analyses of the Model Deposit Fractions Collected from HPLC

Several fractions were collected from HPLC separation. Only two of those fractions are concentrated enough for analyses. They are the peaks marked with "P2" and "P3" in Fig. 7.

The results of PY/MS analyses give little information. The strong solvent peaks are probably caused by the solvent trapped in the residue of the collected fractions during the sample coating process.

In infrared spectroscopy, as shown in Fig. 8, the difference between two fractions is around  $1675\text{ cm}^{-1}$  which is the region of C=C. P2 obviously contains C=C that may be conjugated with other double bonds or with a ketone group. (38) The peak at  $1260\text{ cm}^{-1}$  in both spectra is interesting because it is buried in a broad band in the spectra of the whole model deposit and of the other extracts. This peak could be assigned to an alcohol or a phenol (38), however, there is no OH stretching absorption on the spectra. The possibility that this peak is due to residual  $\text{CHCl}_3$  from the elution solvent is also ruled out because no absorption occurs right below  $750\text{ cm}^{-1}$  which is a characteristic absorption peak of chloroform. This peak thus could be assigned to an absorption due to C-O stretching.

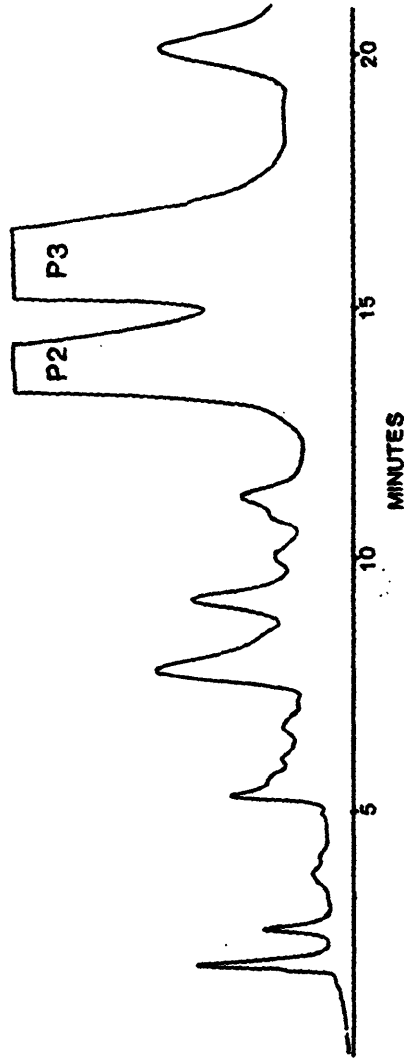


Figure 7 . HPLC Separation of the Model Deposit, P2 and P3 are Two Fractions Collected from the HPLC

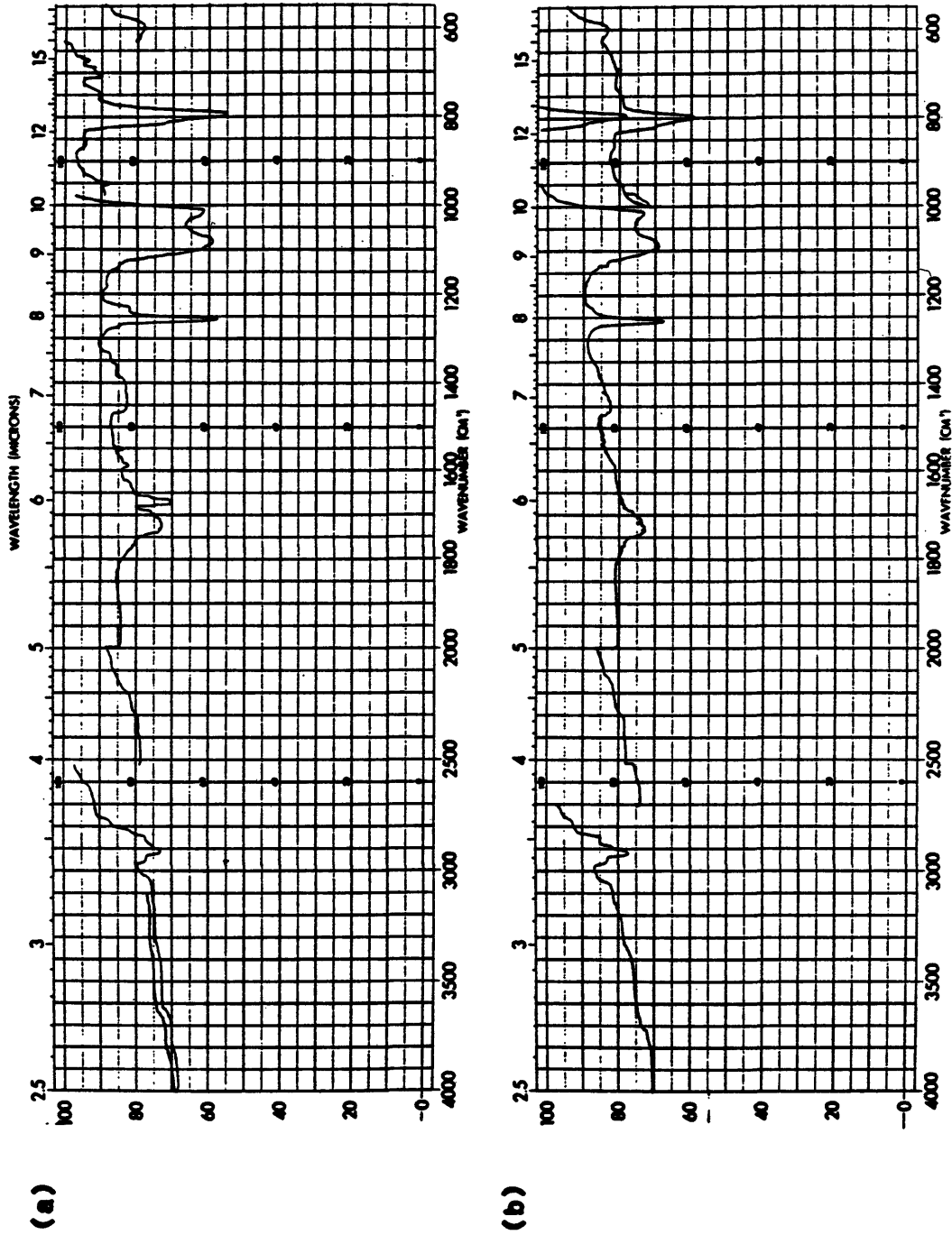


Figure 8 . MIR-IR Spectra of the Model Deposit Fractions Collected from HPLC (a) P2 (b) P3

### Conclusions from MIR-IR Analyses of the Model Deposit

From all the information obtained, the model deposit was concluded to be a mixture rather than a single compound. The compounds in this mixture are mostly aromatic compounds with carbonyl, hydroxyl, or acid functional groups. The carbonyl groups are believed to be from ketones or acids rather than aldehydes because the aldehyde hydrogen is not observed in any IR spectra. The result of wet chemical analyses also show no aldehyde in the model deposit. No definite evidence of the presence of peroxy was found. The saturated ring structure is not well-documented and that could be caused by its association with aromatic rings. Appendix 1 summarizes the IR absorptions for all the analyses of both deposits.

### The Comparison of MIR-IR Analyses of the Benzene Extract and the Benzene-insoluble/THF-soluble Fraction of the Jet A Deposit

In this section, "THF fraction" refers to the fraction, of the Jet A deposit, that is benzene-insoluble but THF-soluble.

In Fig. 9, the benzene extract has a strong C-H stretching peak right below  $3000\text{ cm}^{-1}$  and a weak OH absorption. In contrast, the THF fraction has a stronger OH

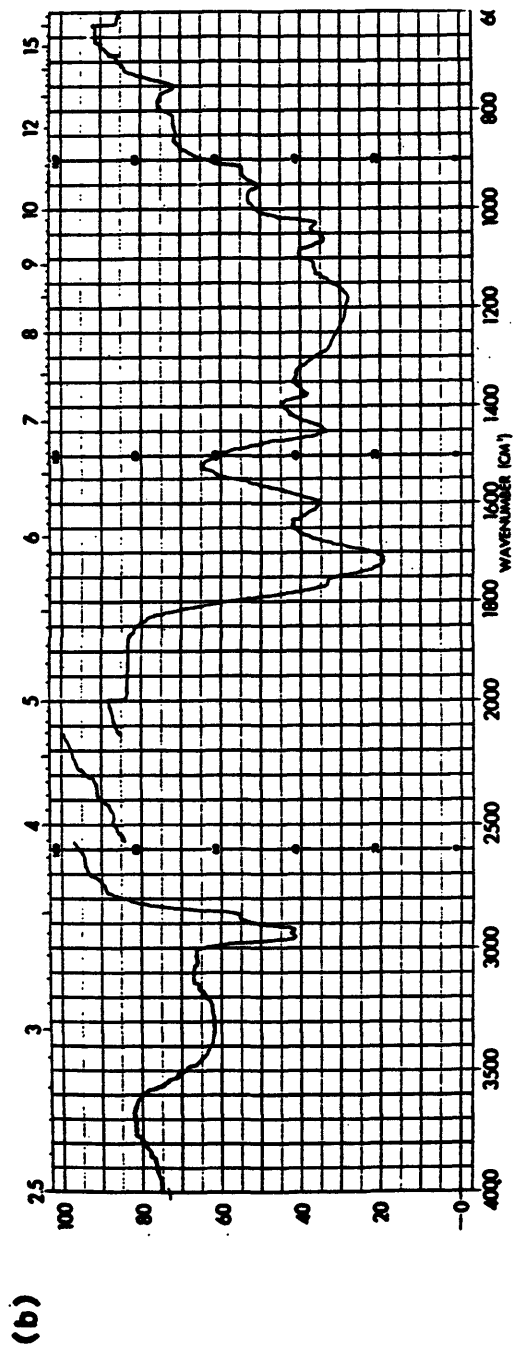
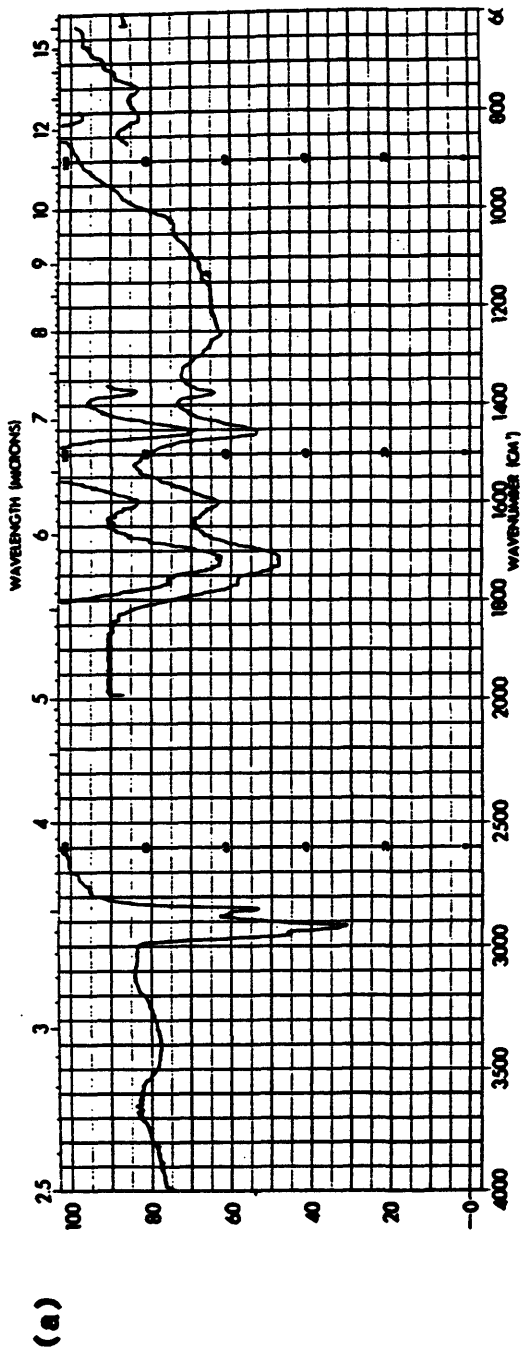


Figure 9. MIR-IR Spectra of the Jet A Deposit  
(a) Benzene Extract (b) THF Fraction

band and a weaker C-H stretching band than does the benzene extract. At  $1050\text{ cm}^{-1}$ , the THF fraction shows a double peak that the benzene extract does not have. The remaining peaks in spectra are very similar except for differences in intensity. The region of  $1050\text{ cm}^{-1}$  is assigned to cyclic ring vibrations. Combining this ring structure with the aromatic features shown in the spectra of both fractions gives support to the conclusions that Jet A deposit contains some compounds with the structure of a saturated ring fused to an aromatic ring. Compounds such as tetralin and its oxidation products are good candidate components of the Jet A deposit.

One comparison which should be noted is that the appearance of the IR spectrum of the model deposit THF fraction and that of the Jet A deposit THF fraction are amazingly similar. Only a slight difference in the region of  $950\text{-}1000\text{ cm}^{-1}$  is seen. This means the polar components in the model deposit have the type of functional groups which also appear in the polar components of the Jet A deposit.

The Comparison of MIR-IR Analyses of the Dichloromethane Extract and the Dichloromethane-insoluble/THF-soluble Fraction of the Jet A Deposit

In this section, "THF fraction" refers to the fraction, of the Jet A deposit, that is dichloromethane-insoluble but THF-soluble.

As shown in Fig. 10, the intensity of C-H stretching in the spectrum of the dichloromethane extract is stronger than that in the spectrum of THF fraction. Another area which shows difference between two spectra is at  $1200\text{ cm}^{-1}$  which could be assigned to the C-O-C stretch of ethers or esters. Since the dichloromethane extract has stronger absorption in this region, these functional groups are probably with the compounds which are dichloromethane soluble and have aliphatic side chains or cyclic structures.

C-13 NMR Spectroscopy (Solution Phase, Deuterated Chloroform as Solvent)

The results of the C-13 liquid state NMR were used only for qualitative interpretation because the experiment was performed, at SERI, in a single run with no knowledge about the relaxation time of the model deposit. Since the model deposit is mixture, its spectrum is very complex.

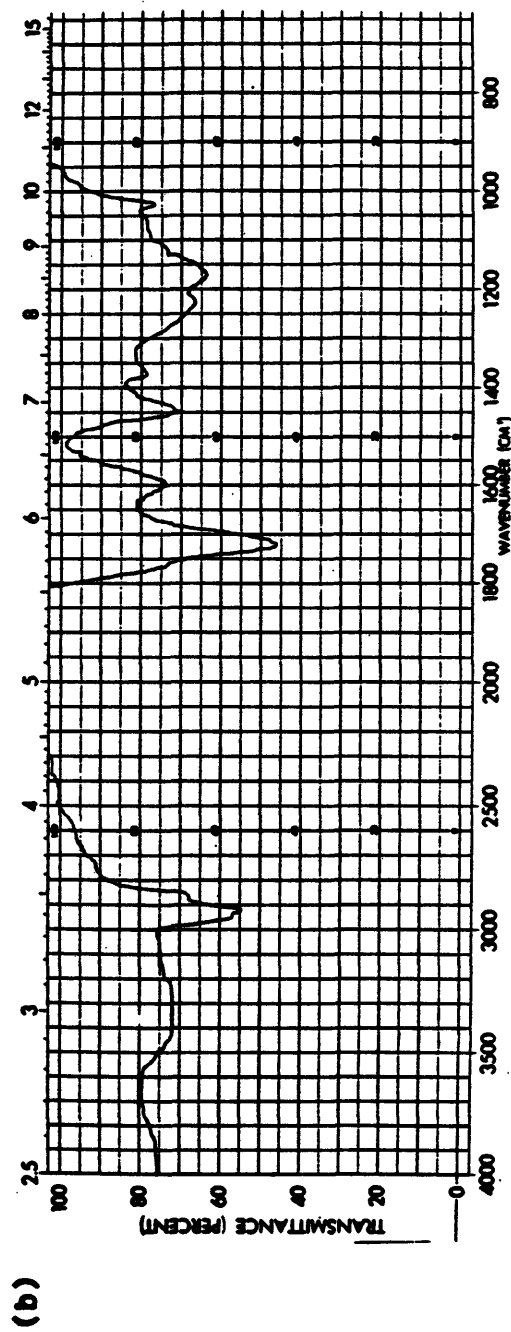
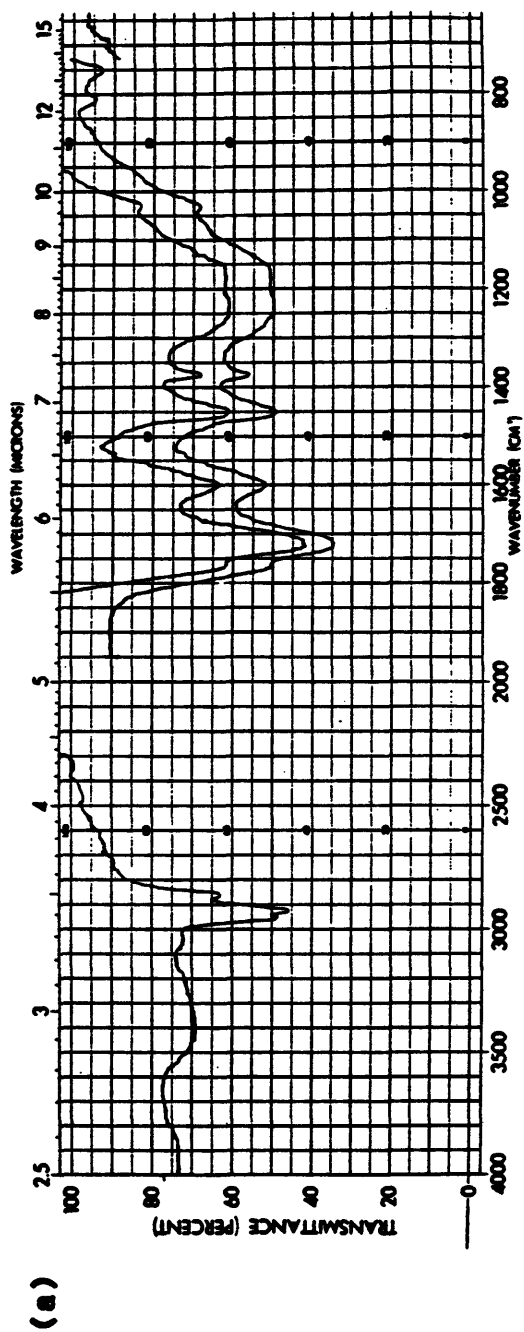


Figure 10. MIR-IR Spectra of the Jet A Deposit  
(a) Dichloromethane Extract (b) THF Fraction

Direct interpretation is difficult and impractical. An attempt was made to extract some information from the spectrum; that is, to compare the spectrum of the model deposit to the spectrum of tetralone found in the literature (39). And in Table 6, the chemical shifts in the spectrum of the model deposit matched with the major chemical shifts of tetralone are listed. The close match of these chemical shifts to the ones of tetralone indicates that the model deposit contains tetralone-like components. The complete C-13 spectrum of the model deposit is in Appendix 2.

#### Proton NMR

Two distinctive groups of peaks are observed in the spectrum of the model deposit (see Fig. 11). One is in the region of 6 - 9 ppm which represents the aromatic hydrogen. Another group appears between 1 ppm and 4 ppm which represents the aliphatic hydrogen region. The ratio of aromatic hydrogen to aliphatic hydrogen was calculated as 1.36 (see Table 7). The spectrum of Jet A deposit is not shown due to the poor quality of the spectrum.

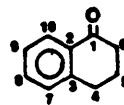
#### CP/MAS Solid State NMR

The integration of different regions of chemical

Table 6. C-13 Chosen Chemical Shifts of the Model Deposit and Tetralone

Carbon No.(a)	Tetralone(b)	Matched Chemical Shifts from Model Deposit(c)
1	197.6	---
2	144.5	144.7
3	132.7	132.7
4	29.6	29.6
5	23.3	23.1
6	39.1	39.0
7	127.0	127.1
8	128.8	128.4
9	133.3	132.7
10	126.5	126.5

a: the carbon numbers are labeled as  
and listed in an decending order of  
intensities



b: obtained from reference 39

c: complete spectrum is in Appendix 2

Table 7. Structural Parameters from NMR Analyses

	Cc=O/Car/Cal	Car/Cal	Har/Hal
Model Deposit (c)	1/11.2/ 4.7	2.38	1.36
Jet A Deposit (c)	1/16.3/15.4	1.06	----
Tetralone (d)	1/ 6 /3	2.00	0.67
Naphtho- quinone (d)	2/ 8 /0	----(a)	----(b)
2,4-dihydro- Naphthoquinone (d)	2/ 6 /2	3.00	1.00

c=O: carbonyl  
ar : aromatics  
al : aliphatics

a: no aliphatic C in the molecular structure  
b: no aliphatic H in the molecular structure  
c: values were calculated from experimental data  
d: values were calculated from the chemical structure

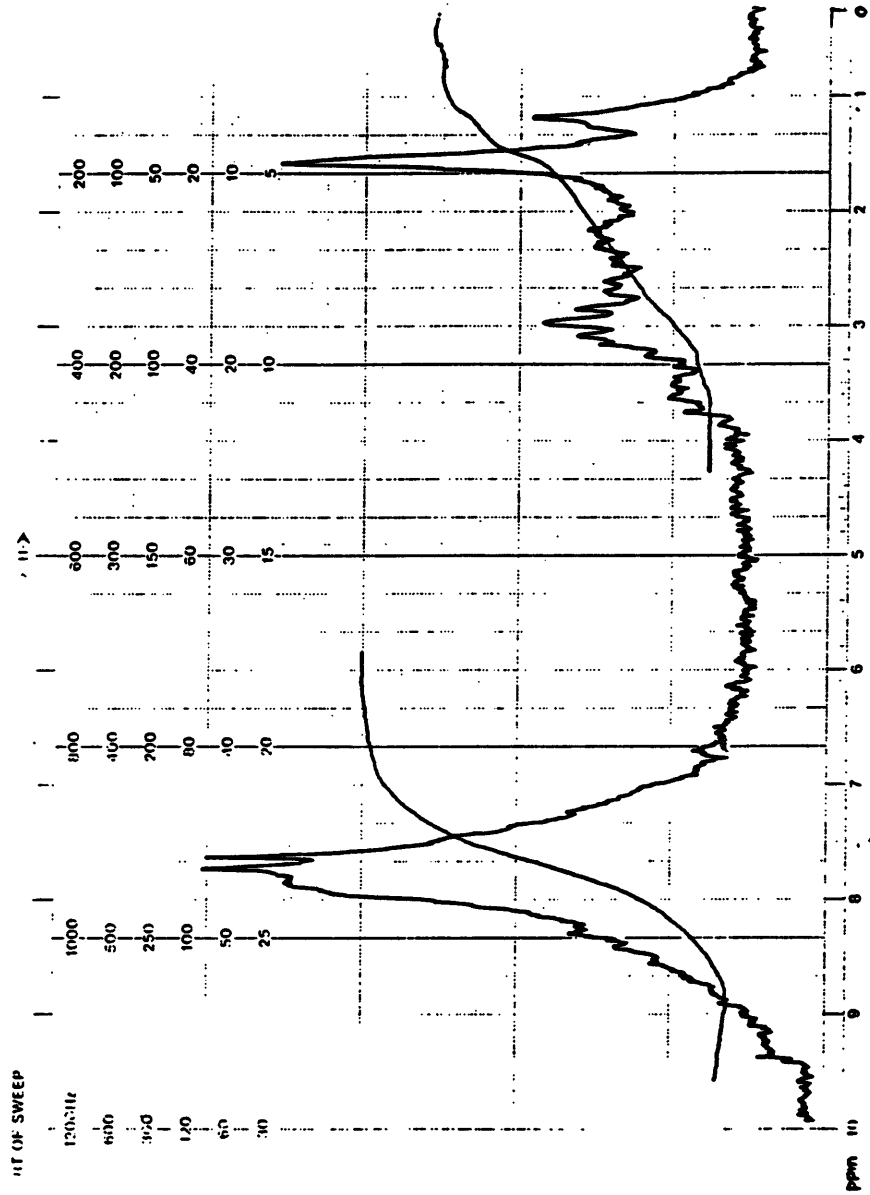


Figure 11. PNMR of the Model Deposit

shift allows the calculation of the ratios among the aliphatic carbons, the aromatic carbons and the carbonyl carbons. These three types of carbons, in the model deposit and in the Jet A deposit, are represented by the integration of 0-50 ppm, 90-160 ppm, and 160-220 ppm (40,41,42) (see Fig. 12 and Fig. 13) respectively. All results, including the data from proton NMR, are listed in Table 7. This table also contains the same type of numbers for some known compounds and the oxidation products of tetralone (35).

For the model deposit, by combining with the CHN data, the aromatic hydrogen to aromatic carbon ratio and aliphatic hydrogen to aliphatic carbon ratio were calculated to be 0.67 and 1.34. Sample calculations are available in Appendix 3. That the aromatic H/aromatic C ratio is less than one indicates fused ring structures or that aromatic rings have substituents. The aliphatic H/ aliphatic C ratio is less than two indicates OH substitution on aliphatic carbons.

### Secondary Ion Mass Spectrometry

The spectrum of the model deposit, Fig. 14, shows peaks over the range up to  $m/e=450$ . The most intensive peak at 73 may be assigned to  $C_4H_9O$ , a fragment from

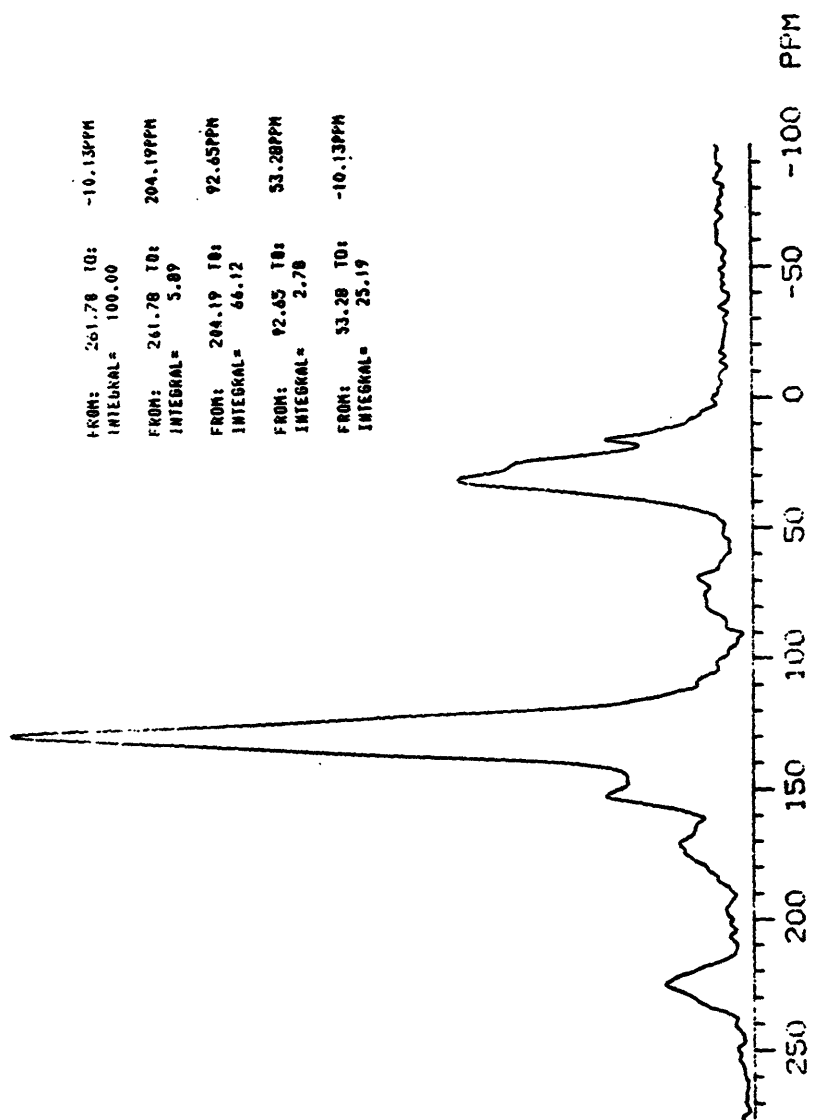


Figure 12. CP/MAS Solid State NMR of the Model Deposit

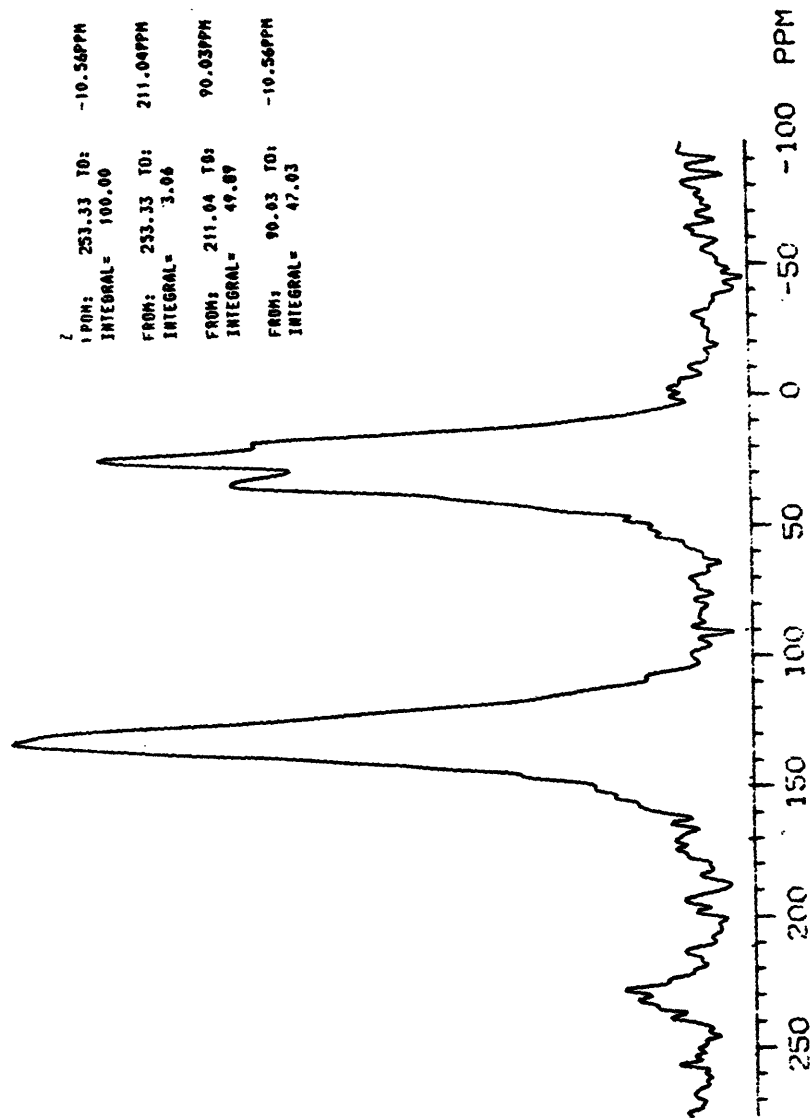


Figure 13. CP/MAS Solid State NMR of the Jet A Deposit

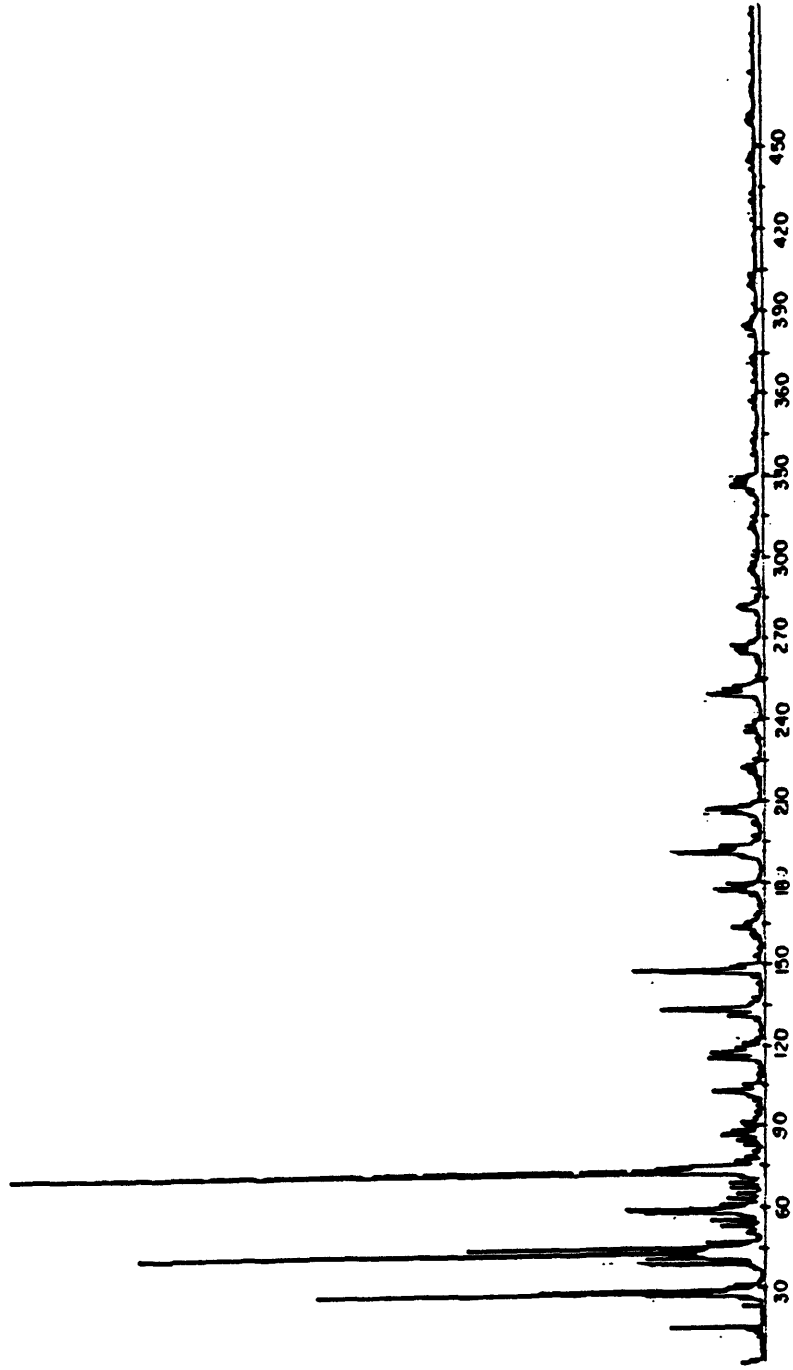


Figure 14. SIMS Spectrum of the Model Deposit

dodecane oxidation products. The peaks at 59 and 45 might be fragments of 73. The peaks appearing around 104 and 118 are possibly fragments from tetralone,  $m/e$  146, by loss of a C=O and a C=C respectively.

The spectrum for the Jet A deposit (Fig. 15) has no peaks above  $m/e=113$ . This result is rather confusing because from GPC data Jet A deposit has an approximate molecular weight of 1000. Major peaks at 23 and 39 represent  $Na^+$  and  $K^+$  from the glass coverslip on which the deposit was coated.

Jet A thermal deposit, received directly from NASA Lewis Research Center, was formed on a aluminum strip. Fig. 16(a) shows the initial spectrum which contains the most intense peak at 73. The second one, Fig. 16(b), is the spectrum after 10 minutes in the spectrometer, it shows a drastic change of the bulk deposit structure from that on the surface. The spectrum then stayed the same after eight hours in the spectrometer. Therefore, the thermal deposit formed on a heated surface has a thin surface layer on top of a thick layer of different material. The surface may be further oxidized after deposit has formed or initially deposited material pyrolyzed on the hot surface. The presence of copper and iron was indicated by the peaks

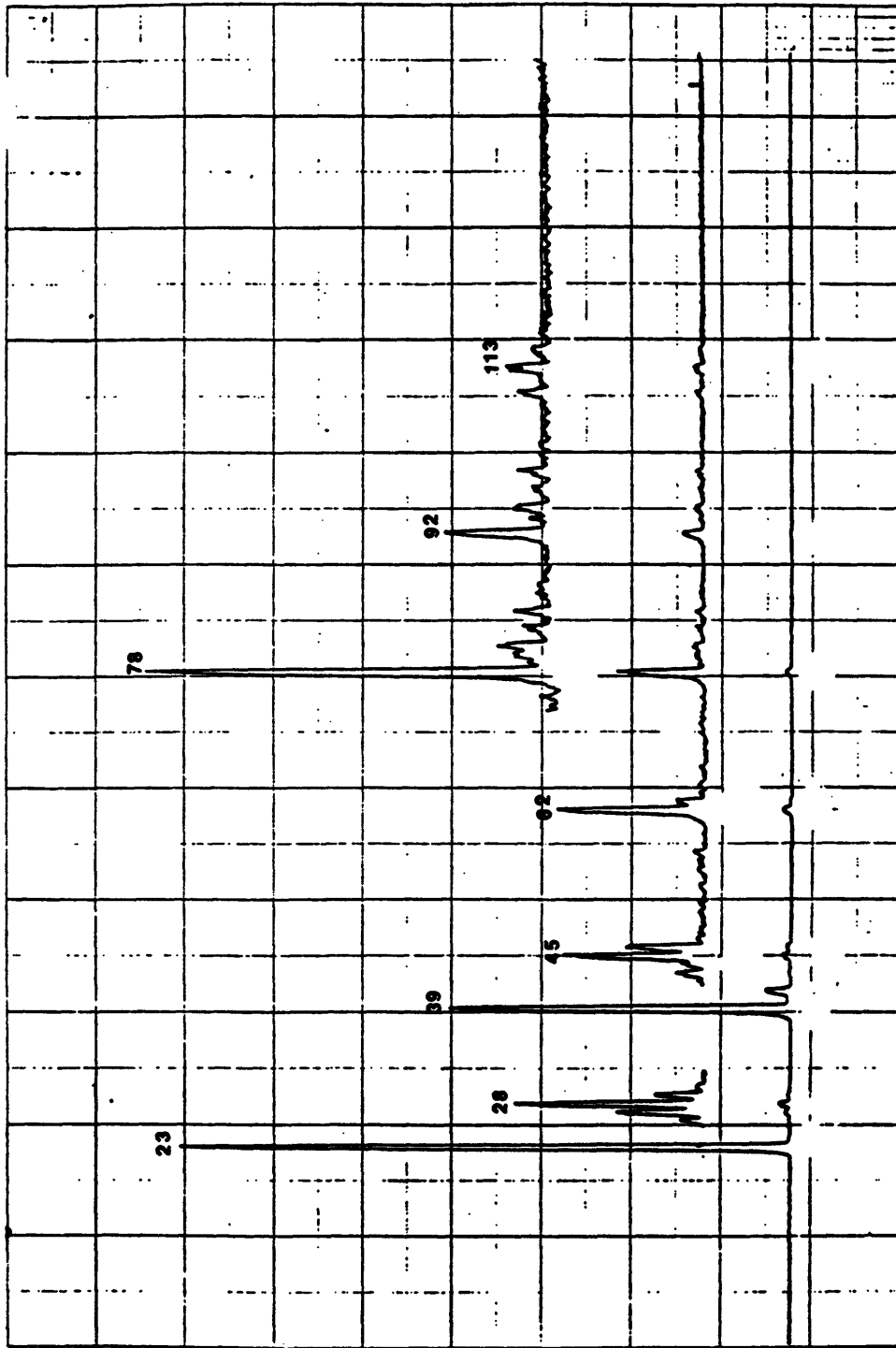


Figure 15. SIMS Spectrum of the Jet A Storage Deposit

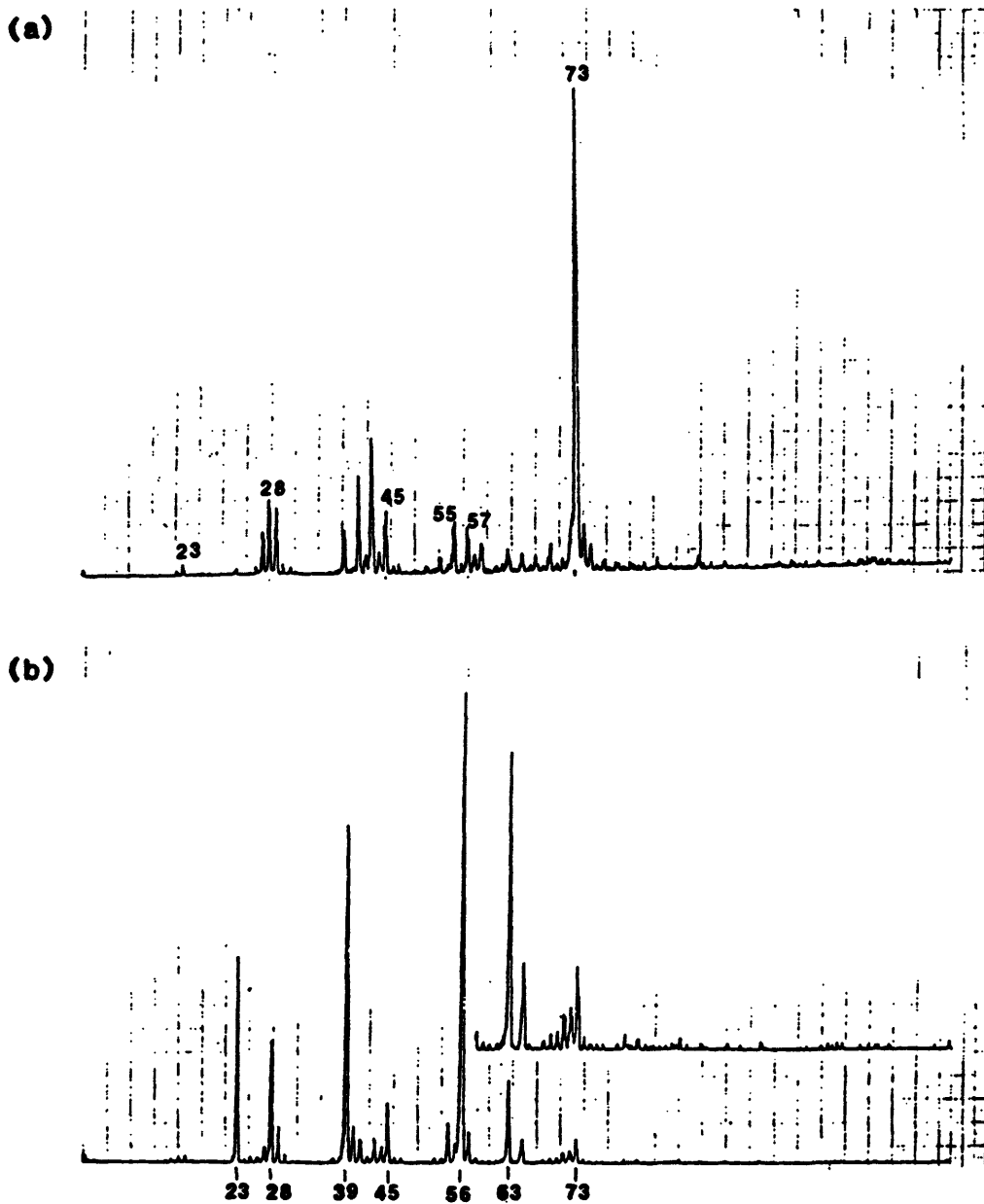


Figure 16. SIMS Spectrum of the Jet A Thermal Deposit  
(a) Initial (b) Final (10 min later)

at 63, 65, and 56.

#### Gas Chromatography/Mass Spectrometry

The fractions obtained from the open column separation (Bond Elute) were analyzed with GC/MS. Tetralone fragments are observed in the benzene fraction of the model deposit. Besides that, very few compounds passed through the GC column. This indicates that the compounds in those fractions are of low volatility either due to polarity or high molecular weight. For this type of sample, PY/MS, is a more powerful source of structural information.

#### Pyrolysis Mass Spectrometric Analyses

The interpretation of PY/MS data is concentrated on fragments rather than molecular ions due to the strong fragmentation tendency of the pyrolysis process. Since the various extracts and fractions are mixtures, identification of individual compounds is extremely difficult. However, comparison of the peak patterns to some standard mass spectra (43) of compounds related to tetralin and its oxidation products provides further understanding of the nature of the model deposit. Table 8 lists the molecular structures that were used for interpretation.

Table 8. The Possible Molecular Structures of the Oxidation Products from Tetralin and Tetralone

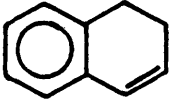
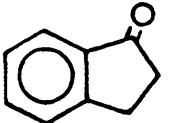
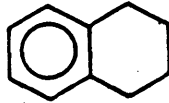
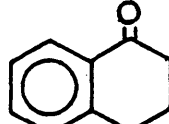
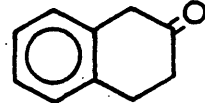
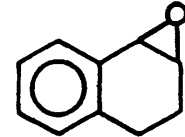
Molecular Structure	Name of Compound
 $C_{10}H_{10}$	1,2-dihydronaphthalene
 $C_9H_8O$	2,3-dihydro-1H-indan-1-one
 $C_{10}H_{12}$	1,2,3,4-tetrahydronaphthalene (Tetralin)
 $C_{10}H_{10}O$	3,4-dihydro-1(2H)-naphthalenone (1-Tetralone)
 $C_{10}H_{10}O$	3,4-dihydro-2(1H)-naphthalenone (2-Tetralone)
 $C_{10}H_{10}O$	1a,2,3,7b-tetrahydronaphth[1,2-b] oxirene

Table 8. (continued)

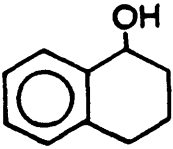
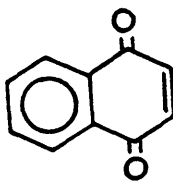
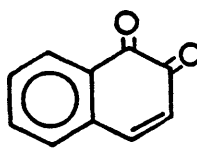
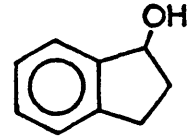
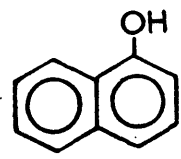
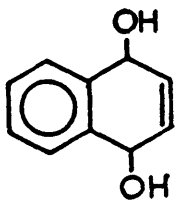
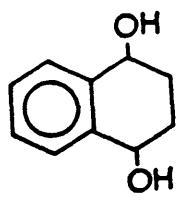
Molecular Structure	Name of CompoundsN
 $C_{10}H_{12}O$	1,2,3,4-tetrahydro-1-naphthalenol (Tetralol)
 $C_{10}H_6O_2$	1,4-naphthoquinone
 $C_{10}H_6O_2$	1,2-naphthoquinone
 $C_9H_{10}O$	2,3-dihydro-1H-indan-1-ol
 $C_{10}H_8O$	1-naphthalenol

Table 8. (continued)

Molecular Structure	Name of Compound
 $C_{10}H_{10}O_2$	1,4-dihydroxynaphthalene
 $C_{10}H_{12}O_2$	1,4-dihydroxytetralin

The solvents used in the extraction processes contribute some peaks in each spectrum. Peaks at 72, 71, 42, and 41 are from THF and the peak at 78 is from benzene. Chloroform contributes to peaks at 83 and 85. Dichloromethane contributes peaks of 84 and 86.

Due to the complexity of pyrolysis processes and the varieties of compounds in the model deposit, each peak in the mass spectrum is expected to have contributions from several sources. Table 9 contains the important peaks of the mass spectra of the chosen compounds shown in Table 8. 1,2-dihydro-naphthalene could be derived from tetralol by loss of  $H_2O$ . It contributes to peaks at 130, 128, and 115. Indanone may also contribute to  $m/e$  130. Indanone is possibly derived from decarboxylation of 1,4-dihydro-Naphthoquinone. Tetralone can lose an ethylene from the 2,3 position to give a peak at 118 or lose a  $H$   $C-CH$  to generate  $m/e=104$  as depicted in Appendix 4 (44). 1-tetralone and 2-tetralone will have the same set of major peaks (146, 118, 104 etc.) except  $m/e=104$  is the strongest peak for 2-tetralone and  $m/e=118$  is the strongest for 1-tetralone. Several higher oxidation products of tetralone (35) may contribute to the spectra.

The number of mass units of every spectrum is limited to four hundred because the spectrum plotting software is

Table 9. Mass Peaks in Spectra of Various Reference Compounds (44)

Compound Name	Molecular Weight	Major Mass Units
1,2-dihydronaphthalene	130	130, 128, 129, 115, 51, 50, 126
2,3-dihydro-1H-indan-1-one	132	130, 114, 113, 131
1,2,3,4-tetrahydro-naphthalene	132	132, 104, 91
3,4-dihydro-1(2H)-naphthalenone	146	146, 118, 90
3,4-dihydro-2(1H)-naphthalenone	146	146, 104, 118, 116
1a,2,3,7b-tetrahydro-naphth[1,2-b]oxirene	146	146, 104, 117, 118, 115, 91, 131
1,2,3,4-tetrahydro-1-naphthalenol	148	130, 120, 91, 119, 148, 147, 105, 116
1,4-naphthalenedione	158	158, 104, 76, 102, 130
1,2-naphthalenedione	158	130, 102, 51, 50, 76
1,2-dihydro-1,2-naphthalenediol	162	116, 115, 149, 118, 76, 90
2,3-dihydro-1H-indan-1-ol	134	133, 134, 115
1-naphthalenol	144	144, 115, 116

written to handle 400 mass units. The high mass portion of the spectrum is not, therefore, shown in spectrum plot because of that limitation. The raw data file of the complete mass units and peak intensities is listed in Appendix 5 for reference.

PY/MS Analyses of the Benzene Extract of the Model Deposit

The spectrum of the benzene soluble fraction, Fig. 17(a), has major peaks at  $m/e=146$ , 130, 120, 118, 115, 104, 78, and 52. The peak at 78 is due to benzene. The mass units 146, 118, and 104 are tetralone fragments. There is no solid evidence to show whether the tetralone is 1- or 2-tetralone because the peaks at 104 and 118 also have contributions from the other compounds. Peaks at 130, 120, 91, and 119 could have contributions from tetralol. Mass unit 130 might also have contributions from 1,2-dihydro-naphthalene, indanone, or 1,2-naphthalenedione. The peak at  $m/e=115$  could be a fragment from 1,2-dihydro-1,2-naphthalenediol, 1,2-dihydro-naphthalene, or 1-naphthalenol.

PY/MS Analyses of the Benzene-insoluble/THF-soluble Fraction of the Model Deposit

In Fig. 17(b), peaks at 71, 72, 42, and 44 are from

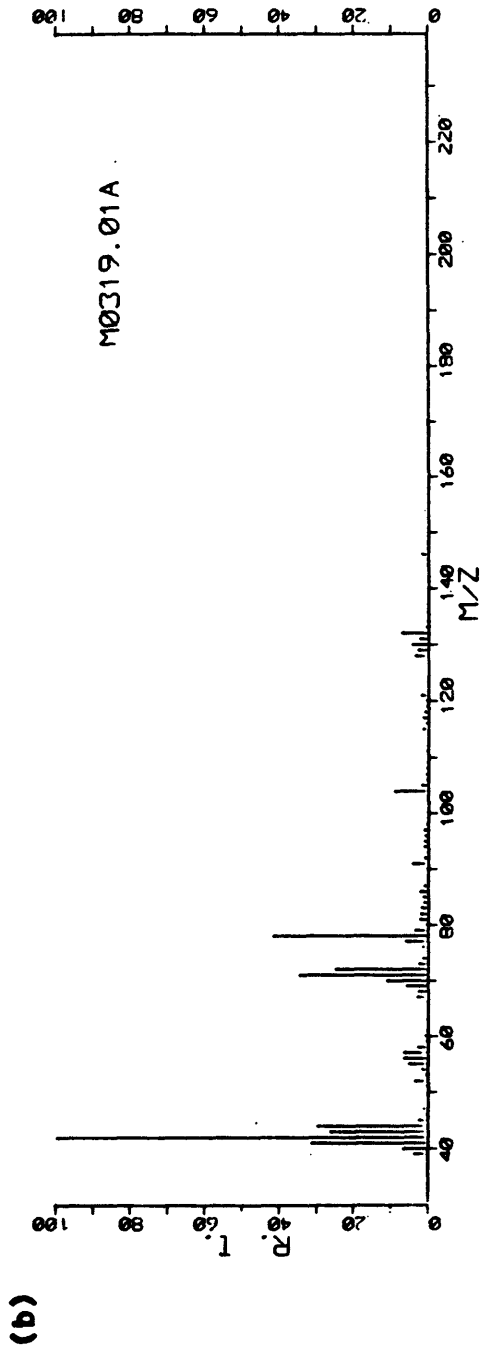
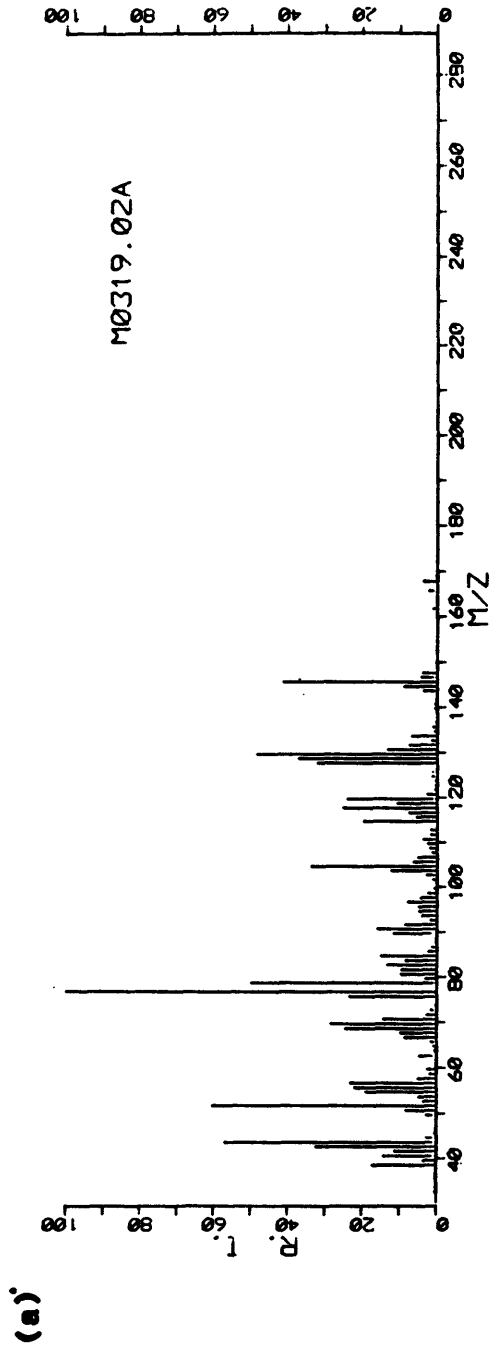


Figure 17. PY/MS Spectra of the Model Deposit  
(a) Benzene Extract (b) THF Fraction

THF and peak at 78 is from benzene. Although the peak intensities are weak, fragments from tetralone are still observable. 2-tetralone might be indicated because the 104 peak is relatively stronger than the 118 peak. The peak at 130 could have contributions from tetralol and some of the other compounds described in the previous section. The mass spectrum of this fraction is similar to that of the benzene extract. The majority of components in this fraction thus have similar structures to those in benzene-soluble fraction but are more polar and not soluble in benzene. One high mass peak,  $m/e=358$ , was found from the raw data file which is not present in the benzene-soluble fraction. The source of that peak is unclear. It could be the parent ion, which is unlikely for pyrolysis, or the source of two or three other fragments.

#### PY/MS Analyses of Benzene Extract of the Jet A Deposit

Surprisingly, the mass spectrum (Fig. 18(a)) shows little similarity to that of the model deposit. The fragments from tetralone are still observable but not significant in the peak intensity. Several clusters of peaks are observed, they are  $m/e=57, 83, 95, 120, 141,$  and  $156$ . Three more peak clusters were found in the raw data file,  $m/e=170, 285,$  and  $362$ . These could be molecular

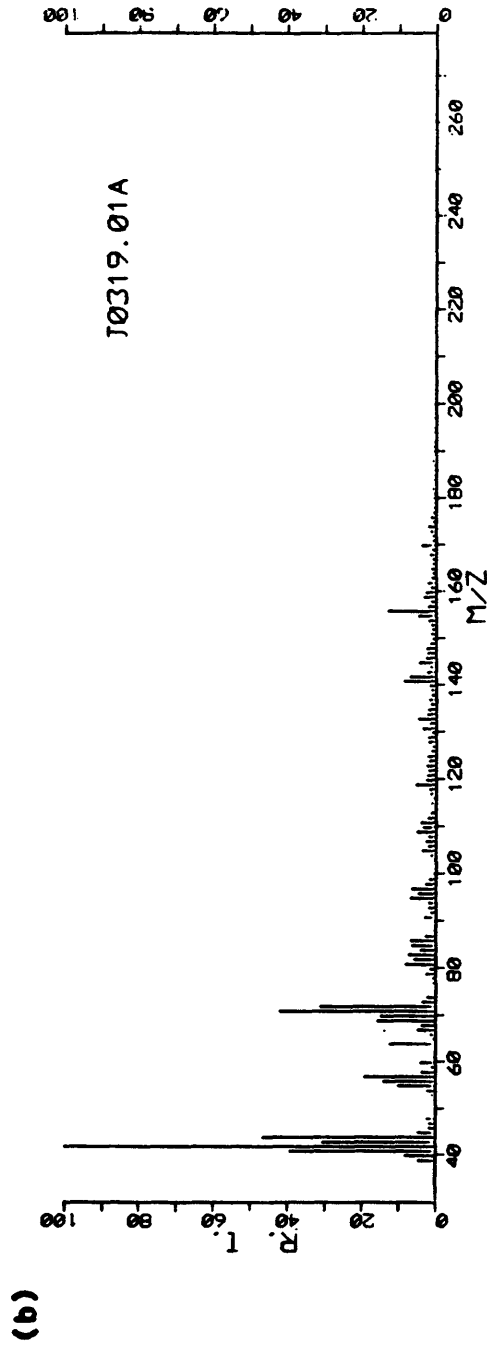
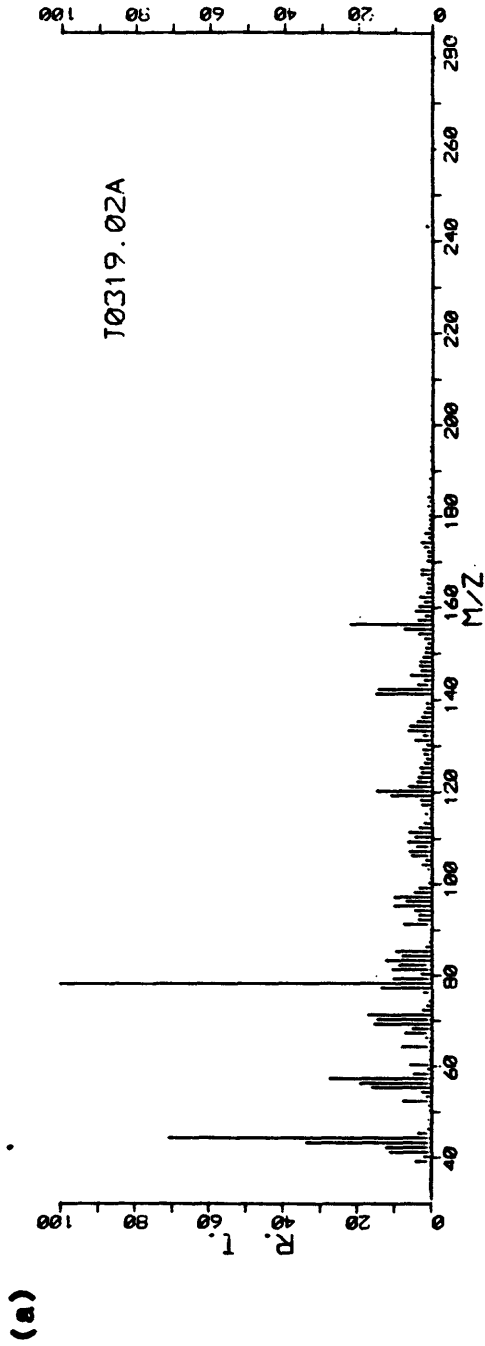


Figure 18. PY/MS Spectra of the Jet A Deposit  
(a) Benzene Extract (b) THF Fraction

ions or the sources of the other fragments.

PY/MS Analyses of the Benzene-insoluble/THF-soluble  
Fraction of the Jet A Deposit

Major peak clusters of this fraction are around  $m/e=384$ , 174/170, 156, 145/146, 141/142, 133, 119/120, 105/109, 95/97, and 81/83 (Fig. 18(b)). There is no good interpretation for the high mass unit 384 because it seems to have no relationship to the other peaks. The peak at 137 may contain an OH and mass unit 119 would be the fragment that lost a  $H_2O$ . The peaks at 156 and 174 as well as the peaks at 141 and 159 could be related in the same way.

PY/MS Analyses of the Dichloromethane Extract of the Model  
Deposit

In Fig. 19(a), mass unit 84, 86, 88, 49 and 51 are from dichloromethane. Not many peaks appear in the spectrum which might be the result of insufficient sample coated on the Curie point wire. Tetralone fragments are present with higher intensity at  $m/e=118$  than at  $m/e=104$ . That is an indication of 1-tetralone. The peak at 90 give a futher support of 1-tetralone because 2-tetralone does not have a distinguishable peak at 90. The mass unit 128

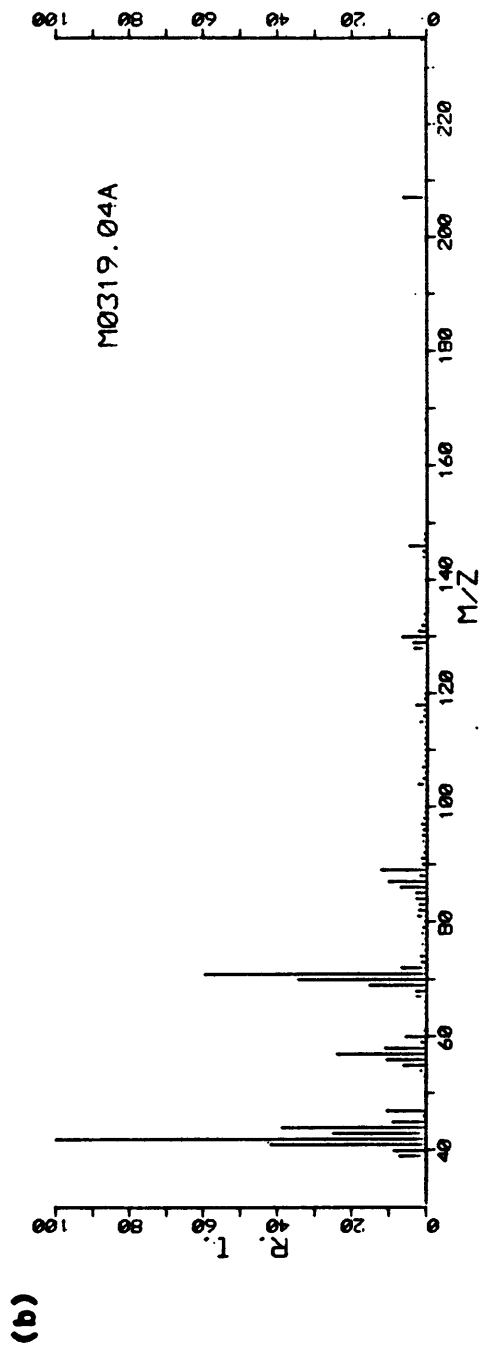
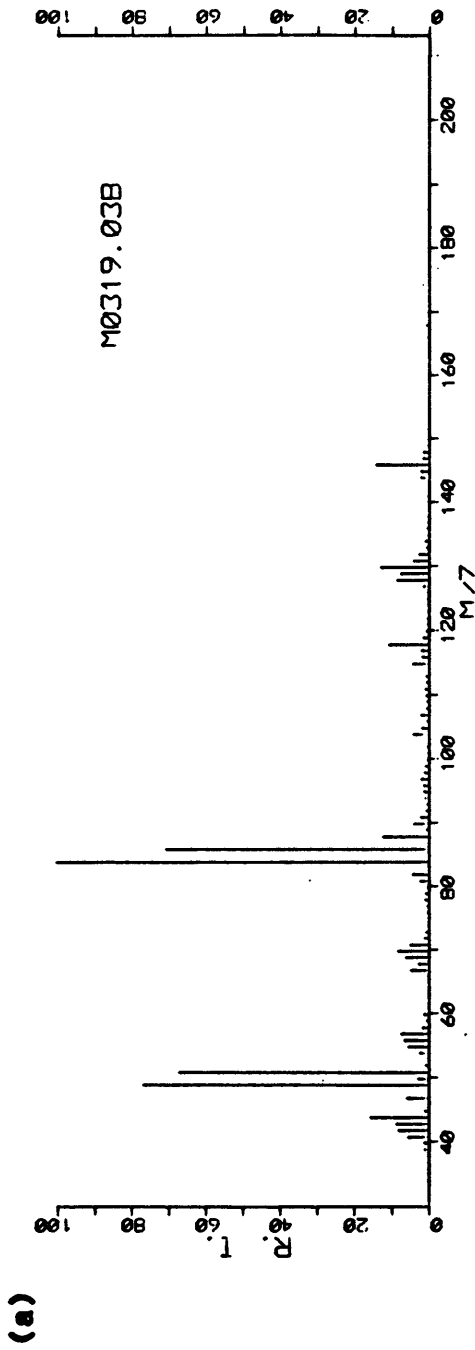


Figure 19. PY/MS Spectra of the Model Deposit  
(a) Dichloromethane Extract (b) THF Fraction

could be naphthalene. The peak at 130 is either from indanone or tetralol. A homologous series, not tetralone derived, might be represented by peaks at 43, 57, and 71. The peak at 115 is related to the peak at 129 by loss of a methyl group. No significant high mass unit was observed by examining the raw data file.

PY/MS Analyses of the Dichloromethane-insoluble/THF-soluble Fraction of the Model Deposit

No peaks are particularly meaningful except the peaks that characterize tetralone (Fig. 19(b)). This indicates most of the components in the model deposit are soluble in dichloromethane. Two higher mass units,  $m/e=207$  and  $339$ , are found above peak 146. The difference between these two mass unit is 132 which could be indane or tetralin. The mass unit 132 must be a neutral species because  $m/e=132$  is not observed in the spectrum.

## CONCLUSIONS

The purpose of this study is to understand more about the structure of the Jet A and model deposits which would provide important information about the mechanism of deposit formation. Unfortunately, the complexity of both systems makes the interpretation of the analytical data extremely difficult. However, this study provides several contributions to the understanding of the structure of both deposits. The following conclusions are drawn from the overall analytical results.

1. The model deposit is concluded to be a mixture because its dichloromethane extract was separated into several components in the HPLC analysis.
2. Tetralone is not directly responsible for the deposit formation but its oxidation products are. The deposit precursors are believed to be the intermediates of the tetralin hydroperoxide decomposition. In other words, oxidation and decomposition of the tetralin hydroperoxide occur simultaneously. This explains why oxygen is required for deposit formation during the tetralin hydroperoxide decomposition process.
3. Peroxy linkages were not found in the model deposit as proposed in the previous work.

4. The compounds comprising model deposit have aromatic-cyclic ring structures with polar functional groups such as carbonyls and alcohols. They are from different combinations of the deposit precursors through condensation reactions.
5. In IR analyses, the Jet A deposit has the same characteristics as model deposit. In PY/MS analyses, however, the Jet A deposit does not show much similarity to the model deposit. That says the two deposits are different in structures but contain the same types of functional groups.
6. On the basis of the PY/MS and C-13 NMR analyses, both 1- and 2-tetralone fragments as well as fragments which don't appear to be derived from tetralin or tetralone are shown. This indicates tetralone-like and aliphatic structures are the "building blocks" of the deposit.
7. In future studies, it is important to understand the oxidation process of tetralone and the mechanism of the decomposition of tetralin hydroperoxide both in oxygen-rich and oxygen-free environments. Also the possibility of the participation of the straight chain alkane (eg. n-dodecane) should be investigated. These experiments could be performed by sealing the reactants

(tetralin hydroperoxide in n-dodecane as a set and tetralone in n-dodecane as another set ) in several sets of vials (nitrogen or oxygen filled) and kept in a 121°C (or other desired temperature) oven. To monitor the reaction, one vial in each set should be removed each 24 hours and then analyzed by GC/MS. After several analyses, a set of characteristic peaks from the gas chromatogram could be chosen to represent the change of the reaction versus time. The identification of those peaks from mass spectra interpretations should provide an insight into the reaction mechanism. If a solid phase formed during the experiment, it could be washed with hexane and fractionated. The solid and its fractions could be analyzed by PY/MS or GC/MS. From these results, the mechanism of the tetralin hydroperoxide decomposition and the tetralone oxidation in n-dodecane would be better understood.

8. In order to determine the molecular weight by GPC, tetralone and its known oxidation products should be used for the calibrations.

## REFERENCES

1. NASA Fuel Stability Group Conference in Cleveland, OH, (1980)
2. R. Hazlett, J. Hall, and J. Solash, ACS Preprint, Div. Fuel Chem., 21, 219 (1976)
3. A. Sachanen, Conversion of Petroleum: Production of Motor Fuels by Thermal and Catalytic Process, Reinhold Publishing Co., New York, p. 117 (1948)
4. F. Mayo, "Chemistry of Fuel Deposits and Sediments and Their Precursors", Final Report Prepared for NASA-Lewis Research Center, October (1981)
5. G. Seng and L. Helmick, Fuel Fundamentals Research Review, NASA Lewis Research Center, p.31, October (1981)
6. CRC Literature Survey on the Thermal Oxidation Stability of Jet Fuel, CRC Report No. 509, Atlanta, Ga., 141 pp (1979)
7. D. Flood, J. Hladky, and G. Edgar, Ind. Eng. Chem., 25, 1234 (1933)
8. J. Morrell, C. Dryer, C. Lowry, and G. Egloff, Ind. Eng. Chem., 26, 497 (1934)
9. J. Morrell, C. Dryer, C. Lowry, and G. Egloff, Ind. Eng. Chem., 28, 465 (1936)
10. A. Tobolsky and R. Mesrobian, Organic Peroxides: Their Chemistry, Decomposition, and Role in Polymerization, Interscience Publishers, Inc., New York (1954)
11. E. Hawkins, Organic Peroxides: Their Formation and Reactions, D. Van Nostrand Co., Inc., Princeton, NJ (1961)
12. K. Ingold, Accounts of Chem. Research, 2, 1 (1969)
13. F. Mayo, Accounts of Chem. Research, 1, 193 (1968)

14. J. Wostell, The Effect of Nitrogen Compounds on Jet A and Diesel Fuels, (Doctoral Thesis-2280-Colorado School of Mines), 141 pp (1980)
15. F. Nayo, "The Chemistry of Fuel Deposits and Their Precursors", Final Report Prepared for NASA, December (1972)
16. F. Taylor, "Fundamental Synthetic Fuel Stability Study", Final Report DOE/BC/10045-20, p. 51-61 (1981)
17. L. Jones, R. Hazlett, N. Li, and J. Ge, ACS, Div. of Fuel Chem. Preprints, 28, 196 (1983)
18. J. Lauer, "Fuel Fundamentals Research Review", NASA Lewis Research Center, Cleveland, OH. p. 79-92 (1983)
19. R. Day, S. Unger, and R. Cooks, Anal. Chem., 52, 557A, (1980)
20. H. Grade, and R. Cooks, J. Am. Chem. Soc., 100, 5615, (1978)
21. A. Benninghoven, and W. Sichterman, Anal. Chem., 50, 1811 (1978)
22. G. Muller, Appl. Phys., 10, 317 (1976)
23. H. Werner, Mikrochimica Acta, Suppl. 7., p. 63 (1977)
24. S. Scheiffers, R. Hollar, K. Busch, and R. Cooks, Am. Lab., p. 19, March (1982)
25. D. VanderHart and H. Retcofsky, Preprint of 1976 Coal Chemistry Workshop held Aug. 26, 1976 at Standford Research Institute, Menlo Park, Ca., p. 202 (1976)
26. V. Bartuska and G. Maciel, Preprint of 1976 Coal Chemistry Workshop held Aug. 26, 1976 at Standford Research Institute, Menlo Park, CA., p. 220 (1976)
27. G. Levy, R. Lichter, and G. Nelson, "Carbon-13 Nuclear Magnetic Resonance Spectroscopy", 2nd Ed., John Wiley & Sons, New York, 338 pp (1980)
28. A. Pines, M. Gibby and J. Waugh, J. Chem. Phys. 59, 569 (1973)

29. R. Griffin, *Anal. Chem.*, 49, 951A (1977)
30. V. Bartuska, G. Maciel, J. Schaefer and E. Stejskal, *ACS, Coal Symposium*, 220 (1979)
31. P. Wilks, Jr., *Am. Lab.*, p. 92, June (1980)
32. Personal communication with Dr. D. Anders at USGS in Denver, Co. (1983)
33. R. Shriner, R. Fuson, and D. Curtin, "The Systematic Identification of Organic Compounds", 5th Ed., John Wiley & Sons, Inc., New York, 458 pp (1964)
34. R. Adams, J. Johnson, and C. Wilcox Jr., *Laboratory Experiments in Organic Chemistry*, 5th ed., Macmillan Co., NY, 560 pp (1963)
35. M. Martan, J. Manaxxen, and D. Vofsi, *Tetra.*, 26, 3815 (1970)
36. Personal communication with K. Zarrabi at the Department of Chemistry in Colorado School of Mines, Golden, CO.
37. *CRC Handbook of Tables for Organic Compound Identification*, CRC Press Inc., p. 170-182 (1980)
38. J. Lambert, H. Shurvell, L. Verbit, R. Cooks, and G. Stout, "Organic Structure Analysis", Macmillan Publishing Co., Inc., London, p. 187-250 (1976)
39. V. Formacek and L. Desnoyer, *C-13 Data Bank*, Vol. 1, p. 451, Bruker Physik, West Germany (1976)
40. R. Botto, and R. Winans, *Fuel*, 62, 271 (1983)
41. G. Gary, *Anal. Chem.*, 47, 546A (1975)
42. C. Johnson, D. Fink, and A. Nixon, *Ind. Eng. Chem.*, 46, 2166 (1954)
43. G. Dinneen and W. Bickel, *Ind. Eng. Chem.*, 43, 1604 (1951)
44. A Cornu and R. Massot, "Compilation of Mass Spectral Data", 2nd ed., 1, 116 (1975)

APPENDICES

Appendix 1. The Summary of the MIR-IR Analyses of the Deposits

A. Model Deposit

MD(a)	MD BENZENE	MD THF(b)	MD CH <sub>2</sub> CL <sub>2</sub>	MD THF(c)	MD P2(d)	MD P3(d)
3330(Br)	3330(Br)	3330(Br)	3330(Br)	3330(Br)	2920	2920
3050	3060	2950	3050	2920(Wk)	1720	1730
2920	2920	2920	2920	1710	1670	1255
2850(Sh)	2850	2860(Sh)	2850(Sh)	1595	1550(Wk)	1090
1700	2640	1760(Sh)	1700	1570(Sh)	1590(Wk)	1015
1625(Wk)	1700	1710	1625(Wk)	1450	1255	795
1590	1630(Sh)	1600	1590	1370	1230(Wk)	600
1570	1590	1450	1570	1250(Br)	1080	
1500	1570	1370	1500	750	1010	
1480	1500	1200(Br)	1480		795	
1450	1485	1060	1450		590	
1370	1450	1030	1370			
1300-	1370	810(Wk)	1200(Br)			
1100(Br)	1290-	750(Wk)	1075(Db)			
1055	1100(Br)		975			
1075	1070		950			
875	955		875			
805	875(Wk)		805			
750	805		750			
640	750		640			
565	640		560			
	560					

a: model deposit, solid

b: the benzene-insoluble fraction of model deposit

c: the dichloromethane-insoluble fraction of model deposit

d: fraction from HPLC collection for model deposit

Br: broad peak

Db: double peaks

Sh: shoulder peaks

Wk: weak peak

## B. Jet A Deposit

JAD(a)	JAD BENZENE	JAD THF(b)	JAD CH <sub>2</sub> CL <sub>2</sub>	JAD THF(c)
3460-	3400(Wk, Br)	3300(Br)	3400(Br)	3300(Wk, Br)
3140(Br)	2950(Sh)	2950	3300	2950
2920	2920	2920	2920	2920
2850(Sh)	2850	2860(Wk)	2860	2860(Sh)
1700	1760(Sh)	1715	1720	1720
1600	1720	1600	1600	1600
1445	1600	1450	1450	1450
1370	1455	1375	1370	1370
1200(Br)	1300-	1300-	1200(Br)	1225
1025(Wk)	1100(Br)	1100(Br)	1030(wk)	1170
805(Wk)	810	1060	810	1030
745	750	1030	750	
		955		
		915(Wk)		
		750		

a: Jet A deposit, solid

b: the benzene-insoluble fraction of Jet A deposit

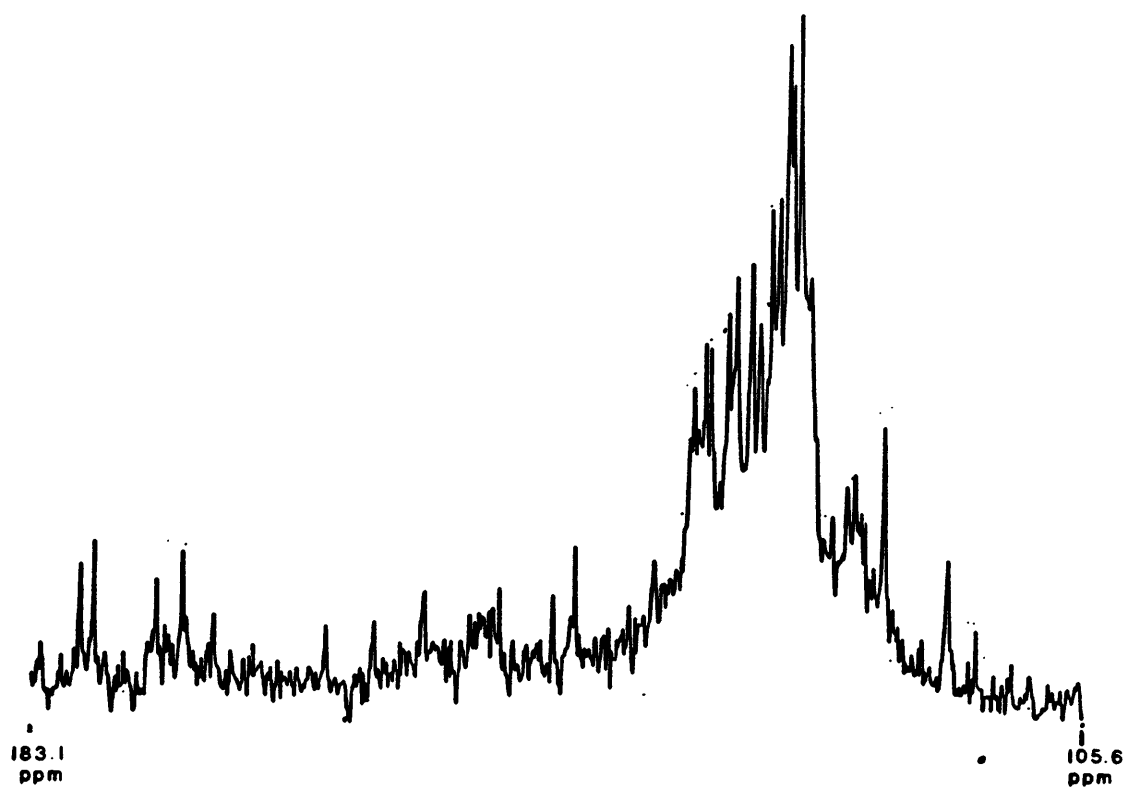
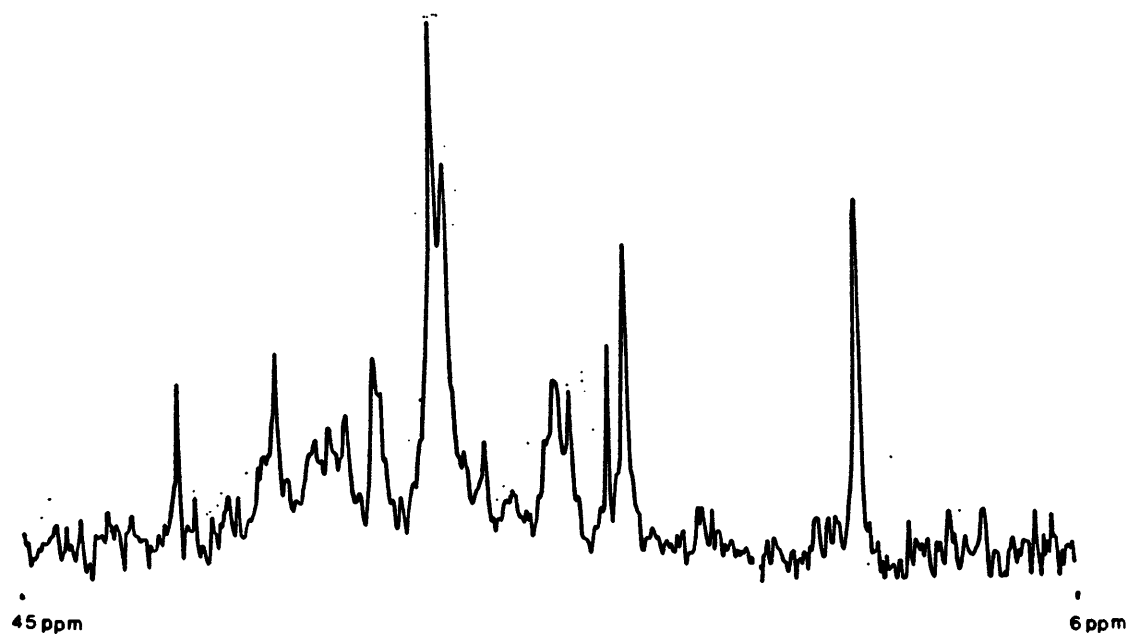
c: the methylene chloride-insoluble fraction of Jet A deposit

Br: broad peak

Sh: shoulder peak

Wk: weak peak

## Appendix 2. C-13 NMR Spectrum of the Model Deposit



## Appendix 3. Sample Calculation of Har/Car and Hal/Cal

Chemical Formula of the Model Deposit  
Derived from CHN Analysis : C<sub>20</sub>H<sub>17</sub>O<sub>4</sub>

Assuming all oxygens are attached to carbon atoms  
then,

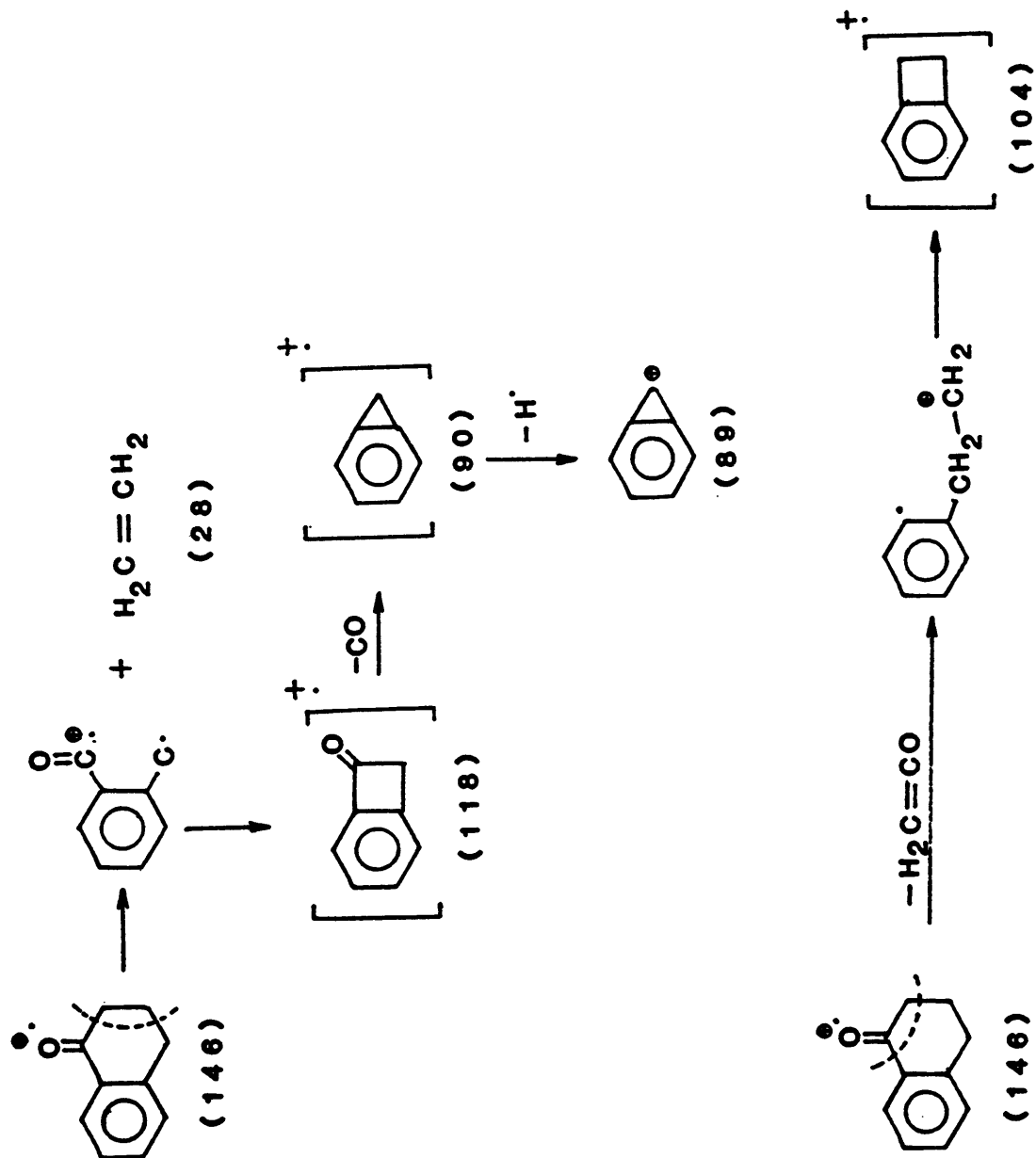
$$\begin{aligned}\# \text{ of C} &= 16 \\ \# \text{ of H} &= 17\end{aligned}$$

From C-13 NMR and H-NMR Analysis, Har/Hal = 1.36  
Car/Cal = 2.38

$$\begin{aligned}\# \text{ of Car} &= [ 16 / (2.38 + 1) ] \times 2.38 = 11.27 \\ \# \text{ of Har} &= [ 17 / (1.36 + 1) ] \times 1.36 = 9.8 \\ \# \text{ of Cal} &= 4.73 \\ \# \text{ of Hal} &= 7.2\end{aligned}$$

$$\begin{aligned}\text{Hal/Cal} &= \# \text{ of Hal} / \# \text{ of Cal} = 1.52 \\ \text{Har/Car} &= \# \text{ of Har} / \# \text{ of Car} = 0.87\end{aligned}$$

Appendix 4. The Mechanism of Tetralone Fragmentation in Mass Spectrometry



Appendix 5. PY/MS Data Files

Model Deposit, Benzene Extract

Mass	RI	Mass	RI	Mass	RI
33	77	87	191	142	57
34	73	88	43	143	62
35	77	89	93	144	77
36	66	90	68	145	23
37	66	91	44	146	17
38	66	92	44	147	37
39	66	93	44	148	37
40	66	94	44	149	37
41	66	95	44	150	37
42	66	96	44	151	37
43	66	97	44	152	37
44	66	98	44	153	37
45	66	99	44	154	37
46	66	100	44	155	37
47	66	101	44	156	37
48	66	102	44	157	37
49	66	103	44	158	37
50	66	104	44	159	37
51	66	105	44	160	37
52	66	106	44	161	37
53	66	107	44	162	37
54	66	108	44	163	37
55	66	109	44	164	37
56	66	110	44	165	37
57	66	111	44	166	37
58	66	112	44	167	37
59	66	113	44	168	37
60	66	114	44	169	37
61	66	115	44	170	37
62	66	116	44	171	37
63	66	117	44	172	37
64	66	118	44	173	37
65	66	119	44	174	37
66	66	120	44	175	37
67	66	121	44	176	37
68	66	122	44	177	37
69	66	123	44	178	37
70	66	124	44	179	37
71	66	125	44	180	37
72	66	126	44	181	37
73	66	127	44	182	37
74	66	128	44	183	37
75	66	129	44	184	37
76	66	130	44	185	37
77	66	131	44	186	37
78	66	132	44	187	37
79	66	133	44	188	37
80	66	134	44	189	37
81	66	135	44	190	37
82	66	136	44	191	37
83	66	137	44	192	37
84	66	138	44	193	37
85	66	139	44	194	37
86	66	140	44	195	37
87	66	141	44	196	37
88	66	142	44	197	37
89	66	143	44	198	37
90	66	144	44	199	37
91	66	145	44	200	37
92	66	146	44	201	37
93	66	147	44	202	37
94	66	148	44	203	37
95	66	149	44	204	37
96	66	150	44	205	37
97	66	151	44	206	37
98	66	152	44	207	37
99	66	153	44	208	37
100	66	154	44	209	37
101	66	155	44	210	37
102	66	156	44	211	37
103	66	157	44	212	37
104	66	158	44	213	37
105	66	159	44	214	37
106	66	160	44	215	37
107	66	161	44	216	37
108	66	162	44	217	37
109	66	163	44	218	37
110	66	164	44	219	37
111	66	165	44	220	37
112	66	166	44	221	37
113	66	167	44	222	37
114	66	168	44	223	37
115	66	169	44	224	37
116	66	170	44	225	37
117	66	171	44	226	37
118	66	172	44	227	37
119	66	173	44	228	37
120	66	174	44	229	37
121	66	175	44	230	37
122	66	176	44	231	37
123	66	177	44	232	37
124	66	178	44	233	37
125	66	179	44	234	37
126	66	180	44	235	37
127	66	181	44	236	37
128	66	182	44	237	37
129	66	183	44	238	37
130	66	184	44	239	37
131	66	185	44	240	37
132	66	186	44	241	37
133	66	187	44	242	37
134	66	188	44	243	37
135	66	189	44	244	37
136	66	190	44	245	37
137	66	191	44	246	37
138	66	192	44	247	37
139	66	193	44	248	37
140	66	194	44	249	37
141	66	195	44	250	37
142	66	196	44	251	37
143	66	197	44	252	37
144	66	198	44	253	37
145	66	199	44	254	37
146	66	200	44	255	37
147	66	201	44	256	37
148	66	202	44	257	37
149	66	203	44	258	37
150	66	204	44	259	37
151	66	205	44	260	37
152	66	206	44	261	37
153	66	207	44	262	37
154	66	208	44	263	37
155	66	209	44	264	37
156	66	210	44	265	37
157	66	211	44	266	37
158	66	212	44	267	37
159	66	213	44	268	37
160	66	214	44	269	37
161	66	215	44	270	37
162	66	216	44	271	37
163	66	217	44	272	37
164	66	218	44	273	37
165	66	219	44	274	37
166	66	220	44	275	37
167	66	221	44	276	37
168	66	222	44	277	37
169	66	223	44	278	37
170	66	224	44	279	37
171	66	225	44	280	37
172	66	226	44	281	37
173	66	227	44	282	37
174	66	228	44	283	37
175	66	229	44	284	37
176	66	230	44	285	37
177	66	231	44	286	37
178	66	232	44	287	37
179	66	233	44	288	37
180	66	234	44	289	37
181	66	235	44	290	37
182	66	236	44	291	37
183	66	237	44	292	37
184	66	238	44	293	37
185	66	239	44	294	37
186	66	240	44	295	37
187	66	241	44	296	37
188	66	242	44	297	37
189	66	243	44	298	37
190	66	244	44	299	37
191	66	245	44	300	37
192	66	246	44	301	37
193	66	247	44	302	37
194	66	248	44	303	37
195	66	249	44	304	37
196	66	250	44	305	37
197	66	251	44	306	37
198	66	252	44	307	37
199	66	253	44	308	37
200	66	254	44	309	37
201	66	255	44	310	37
202	66	256	44	311	37
203	66	257	44	312	37
204	66	258	44	313	37
205	66	259	44	314	37
206	66	260	44	315	37
207	66	261	44	316	37
208	66	262	44	317	37
209	66	263	44	318	37
210	66	264	44	319	37
211	66	265	44	320	37
212	66	266	44	321	37
213	66	267	44	322	37
214	66	268	44	323	37
215	66	269	44	324	37
216	66	270	44	325	37
217	66	271	44	326	37
218	66	272	44	327	37
219	66	273	44	328	37
220	66	274	44	329	37
221	66	275	44	330	37
222	66	276	44	331	37
223	66	277	44	332	37
224	66	278	44	333	37
225	66	279	44	334	37
226	66	280	44	335	37
227	66	281	44	336	37
228	66	282	44	337	37
229	66	283	44	338	37
230	66	284	44	339	37
231	66	285	44	340	37
232	66	286	44	341	37
233	66	287	44	342	37
234	66	288	44	343	37
235	66	289	44	344	37
236	66	290	44	345	37
237	66	291	44	346	37
238	66	292	44	347	37
239	66	293	44	348	37
240	66	294	44	349	37
241	66	295	44	350	37
242	66	296	44	351	37
243	66	297	44	352	37
244	66	298	44	353	37
245	66	299	44	354	37
246	66	300	44	355	37
247	66	301	44	356	37
248	66	302	44	357	37
249	66	303	44	358	37
250	66	304	44	359	37
251	66	305	44	360	37
252	66	306	44	361	37
253	66	307	44	362	37
254	66	308	44	363	37
255	66	309	44	364	37
256	66	310	44	365	37
257	66	311	44	366	37
258	66	312	44	367	37
259	66	313	44	368	37
260	66	314	44	369	37
261	66	315	44	370	37
262	66	316	44	371	37
263	66	317	44	372	37
264	66	318	44	373	37
265	66	319	44	374	37
266	66	320	44	375	37
267	66	321	44	376	37
268	66	322	44	377	37
269	66	323	44	378	37
270	66	324	44	379	37
271	66	325	44	380	37
272	66	326	44	381	37
273	66	327	44	382	37
274	66	328	44	383	37
275	66	329	44	384	37
276	66	330	44	385	37







Jet A Deposit, Benzene Extract

Mass	RI	Mass	RI	Mass	RI	Mass	RI
111	1	111	1	111	1	111	1
112	1	112	1	112	1	112	1
113	1	113	1	113	1	113	1
114	1	114	1	114	1	114	1
115	1	115	1	115	1	115	1
116	1	116	1	116	1	116	1
117	1	117	1	117	1	117	1
118	1	118	1	118	1	118	1
119	1	119	1	119	1	119	1
120	1	120	1	120	1	120	1
121	1	121	1	121	1	121	1
122	1	122	1	122	1	122	1
123	1	123	1	123	1	123	1
124	1	124	1	124	1	124	1
125	1	125	1	125	1	125	1
126	1	126	1	126	1	126	1
127	1	127	1	127	1	127	1
128	1	128	1	128	1	128	1
129	1	129	1	129	1	129	1
130	1	130	1	130	1	130	1
131	1	131	1	131	1	131	1
132	1	132	1	132	1	132	1
133	1	133	1	133	1	133	1
134	1	134	1	134	1	134	1
135	1	135	1	135	1	135	1
136	1	136	1	136	1	136	1
137	1	137	1	137	1	137	1
138	1	138	1	138	1	138	1
139	1	139	1	139	1	139	1
140	1	140	1	140	1	140	1
141	1	141	1	141	1	141	1
142	1	142	1	142	1	142	1
143	1	143	1	143	1	143	1
144	1	144	1	144	1	144	1
145	1	145	1	145	1	145	1
146	1	146	1	146	1	146	1
147	1	147	1	147	1	147	1
148	1	148	1	148	1	148	1
149	1	149	1	149	1	149	1
150	1	150	1	150	1	150	1
151	1	151	1	151	1	151	1
152	1	152	1	152	1	152	1
153	1	153	1	153	1	153	1
154	1	154	1	154	1	154	1
155	1	155	1	155	1	155	1
156	1	156	1	156	1	156	1
157	1	157	1	157	1	157	1
158	1	158	1	158	1	158	1
159	1	159	1	159	1	159	1
160	1	160	1	160	1	160	1
161	1	161	1	161	1	161	1
162	1	162	1	162	1	162	1
163	1	163	1	163	1	163	1
164	1	164	1	164	1	164	1
165	1	165	1	165	1	165	1
166	1	166	1	166	1	166	1
167	1	167	1	167	1	167	1
168	1	168	1	168	1	168	1
169	1	169	1	169	1	169	1
170	1	170	1	170	1	170	1
171	1	171	1	171	1	171	1
172	1	172	1	172	1	172	1
173	1	173	1	173	1	173	1
174	1	174	1	174	1	174	1
175	1	175	1	175	1	175	1
176	1	176	1	176	1	176	1
177	1	177	1	177	1	177	1
178	1	178	1	178	1	178	1
179	1	179	1	179	1	179	1
180	1	180	1	180	1	180	1
181	1	181	1	181	1	181	1
182	1	182	1	182	1	182	1
183	1	183	1	183	1	183	1
184	1	184	1	184	1	184	1
185	1	185	1	185	1	185	1
186	1	186	1	186	1	186	1
187	1	187	1	187	1	187	1
188	1	188	1	188	1	188	1
189	1	189	1	189	1	189	1
190	1	190	1	190	1	190	1
191	1	191	1	191	1	191	1
192	1	192	1	192	1	192	1
193	1	193	1	193	1	193	1
194	1	194	1	194	1	194	1
195	1	195	1	195	1	195	1
196	1	196	1	196	1	196	1
197	1	197	1	197	1	197	1
198	1	198	1	198	1	198	1
199	1	199	1	199	1	199	1
200	1	200	1	200	1	200	1

RI: Relative Intensity

